rijksuniversiteit groningen

Intrinsic self-healing thermosetting nanocomposites based on physical and thermally-reversible linkages

by

Dian S. Santosa

Submitted in partial fulfilment of the requirements for the degree of

Master of Science in Chemical Engineering

Department of Chemical Engineering
Faculty of Mathematics and Natural Science
University of Groningen
July 2016

Justification

Title:	Intrinsic self-healing thermosetting nanocomposites based on physical and thermally-reversible linkages
Status:	Final Version
Date of Publication:	13 / 07 / 2016
Author:	Dian S. Santosa

Contact:	Dian S. Santosa
E-mail:	d.s.santosa@student.rug.nl
Student #:	S2528533
Institution:	University of Groningen
Faculty:	Faculty of Mathematics and Natural Sciences
Department:	Chemical Engineering
Address:	Nijenborgh 4, 9747 AG Groningen
Thesis Assessors:	Prof. dr. F. Picchioni
	dr. P.P. Pescarmona
Supervisors:	dr. P. Raffa
	R.A. Araya-Hermosilla, M.Sc.

Acknowledgement

The journey to finish this project – and by extension, my study – has not always been a smooth sailing; there were many obstacles both foreseen and unforeseen. In the end however, all of them have been overcome, although that would not have been possible if it were not for the assistance and guidance of the people I'm naming on this page, and many more.

First of all, I would like to thank my parents, brothers and aunt which have always been the source constant motivation support, urging me to follow my dream to go abroad and further my study and reminding me of my purpose when I started to have doubts.

Another person I would greatly thank for the completion of this project is Prof. dr. Francesco Picchioni whom, despite an initially unimpressive performance I've shown in his class, still chose to give me the opportunity to be a part of the research group and work on this particular project.

Secondly, I would like to sincerely thank dr. Patrizio Raffa and Rodrigo A. Araya-Hermosilla, M.Sc. for their willingness to guide and give feedbacks throughout the project, giving hints and insight on parts that I would've missed otherwise. I'm aware that I wasn't the easiest person to work with, and I truly appreciate both of you making time to help me finish the project.

Thirdly, I would like to express my gratitude to the people who are not a part of the project in a formal way, but have helped me immensely during the course of the work. They are, in no particular order: ir. L. M. Polgar; M. Beljaars, M.Sc.; Susanti, M.Sc.; I. Gavrila, M.Sc.; A.J. Kamphuis, M.Sc.; A.P. Kristijarti, S.Si, M.T.; R.M. Abdilla; ing. E. Wilbers; M.H. de Vries; A. Appeldoorn; ing. M. Stookroos; ir. S. Achterop; ing. J.H. Marsman; ing. L. Rohrbach; and E.A. Araya-Hermosilla.

Thank you so much as well to E. Frankes and A.A. Frankes-Purwanto for letting me stay with them when I was about to be evicted from my room. As hard as I try, the troll lifestyle of living under a random bridge does not seem to agree with me nor with the gemeente's rule for vagabonds.

And at last, but not least, I would extend my gratitude to my friends: K. Healy, K. Aves, J. Riihimäki, O. Lê, M. Goncalves, S. Matthysen, N. Malinen, L. Daniel, H. Muljana, J. Kabel, J. Hacking, M. Koeslag, J. Paauwe, J.J. Mercadal, and everyone else in the office. Thank you for all the chitchats and jokes, both appropriate and inappropriate.

Abstract

In this thesis, we investigated the intrinsic self-healing property and electrical response of a thermoset nanocomposite containing both covalent, although thermally-reversible, and physical linkages. Previous research into this topic has shown that a similar system based on a polyketone containing both thermally-reversible crosslinks and physical linkages are able to undergo self-healing that is triggered by heat and electricity (via resistive heating). However, this published work did not study further the effect of composition (i.e. the ratio between these two kinds of modified polyketones) on the electrical response and self-healing efficiency.

Thus, the main goal of this thesis was to investigate the influence of different crosslinking density on the self-healing property and electrical response. The influence of different crosslink density was investigated by two means: by changing the degree of functionalization of the polymer backbone and by changing the ratio between polymers containing thermally reversible crosslinks and polymers containing physical links. First, polyketone functionalized with furan (the precursor of thermally reversible linkages via the Diels Alder mechanism) at several predetermined conversion degree was prepared using Paal-Knorr reaction. The materials were then characterized to confirm that the functionalization has reached the desired level.

The functionalization was followed by the nanocomposite preparation, where both types of polyketones were mixed at different ratio and had multi-walled carbon nanotubes (MWCNT) added as reinforcement and electrical conductor. The resulting materials were then tested for its self-healing capability and electrical response at different degree of conversion.

The results from the research confirm what the previous findings: a mixture between polyketone functionalized with furan (precursors for the thermally reversible covalent bonds) and polyketone functionalized with aminopropanol (able to interact via hydrogen bonding, i.e. physical linkages) are able to exhibit self-healing behaviour when exposed to sufficiently high temperature. The presence of MWCNT also allowed the heat to come from electrical source via Joule / resistive heating. Additionally, it was discovered that increasing the amount of polyketones functionalized with furan in a given system results in a composite that has lower electrical resistance, most likely due to the crosslinks that can form between polyketones and MWCNT, allowing better dispersion and reducing the chance for MWCNT to form aggregates.

Table of Contents

1. Introduction

This thesis aims to systematically investigate the intrinsic self-healing property of a thermoset nanocomposite which contains two different types of polyketones: one functionalized with thermally reversible linkage, and the other functionalized with a moiety that can display physical linkages in terms of hydrogen bonding. Additionally, multi-walled carbon nanotubes (MWCNT) were added to act as reinforcement to the polymers and allow for electrical conduction. In turn, the presence of MWCNT allows for the intrinsic self-healing to be triggered by resistive heating once the composite is connected to an electrical source.

The introduction will cover different topics related to the development of the material. A short explanation about polymers and their classification will be addressed and followed with a more detailed information regarding the chosen material: polyketones. Explanation about the chosen materials will be followed by discourses on three important subjects which directly correlate with this thesis: composite materials, interpenetrating polymer network, and self-healing polymers.

1.1 Polymers

Although they are present in almost all lifeforms and have been utilized by various human civilizations since ancient times, the story of modern polymeric materials can be argued to begin when Henri Braconnot and his team developed a derivative of the natural polymer cellulose to produce celluloid in the early 1800s [1]. This was followed by the first notable polymer modification process, which can be traced to Thomas Hancock and Charles Goodyear in 1844 which used sulphur to toughen natural rubber in a process known as vulcanization [2].

Since then, knowledge on the subject of polymers and their industrial application has increased further, with the first fully-synthetic polymer dubbed 'Bakelite' synthesized in 1907 by Leo Baekeland [3]. This invention led to further discoveries of synthetic polymers such as cellulose acetate, polyethylene, and polystyrene [4]. Further interest in synthetic polymers was fuelled by the Second World War, where rationing systems and uncertainties of war limited access to natural polymers for industrial and civilian uses [5]. This led to the development of synthetic polymers with specific properties rather than materials to mimic natural polymers. The new direction resulted in the development of new polymers such as Neoprene (polychloroprene) and Kevlar (poly-paraphenylene terephthalamide) [6,7]. Today, synthetic polymers can be found in almost every modern industrial product and in all sorts of applications.

Polymers can be divided into different classes and multiple categories: according to their thermal processing behaviour, mechanism of polymerization, polymer structure [8], source, and monomer types [9]. Regarding the thermal processing behaviour, polymers can be divided into thermoplastics and thermosets. Thermoplastics are materials that undergo physical changes and become softer and pliable when exposed to temperatures above their glass transition [10]. On the other hand, thermosets are polymers that irreversibly change from soft solid or viscous state into infusible and insoluble polymer networks after curing [11]. The previously-mentioned vulcanization, for example, is a process which turns a thermoplastic biopolymer (e.g. natural rubber) into a thermoset.

1.2 Polyketones

As previously mentioned, this thesis will deal primarily with polyketones, a polymer first synthetized by Farbenfabriken Bayer in 1941, where ethylene and carbon monoxide were polymerized by free radical polymerization under 400 bar pressure at 250 °C, resulting in a randomly-distributed polymer [12]. The process was further improved by the production of low-melting polyketone oligomers by

Reppe and Magin utilizing $K_2Ni(CN)_4$ as catalyst in the late 1940s (Figure 1) [13]; development of palladium(II) catalyst by A. Gough from the now-defunct Imperial Chemical Industries, Ltd in 1967; and finally improvement of the palladium catalyst by Shell in 1983 which was followed by the commercial release of Carilon® polyketone in 1996 [14].

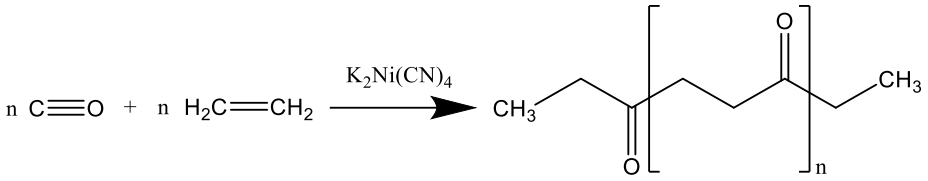

Figure 1. Alternating ethylene-carbon monoxide polyketone. The reaction is based on the work published by Reppe & Magin [15]

The primary advantage of modern polyketones is the ease of manufacture: the introduction of palladium bidentate catalyst from Shell allows the production of polyketones under relatively mild conditions of pressure (50-60 bar) using temperatures ranged from 70-135 °C [16]. Aside from that, polyketone has gained a lot of attraction due to: availability of base materials, relatively cheap cost of production, and interesting engineering plastic properties[15].

Academic research into polyketone and its derivatives have been revitalized within the last 10 years [17]. Polyketone has been modified to produce polymeric amines [17], self-healing polymeric materials [18], wood adhesive [19], biocompatible polymer [20], and even shape-memory elastomers [21].

Previous research showed that functionalization of perfectly alternating polyketone can be easily carried out due to the presence of highly reactive 1,4 di-carbonyl groups [17]. The simplest modification of this chemical group can be done by Paal-Knorr reaction (Figure 2), commonly used to carry out the chemical modification of polyketone with amine compound [21-23].

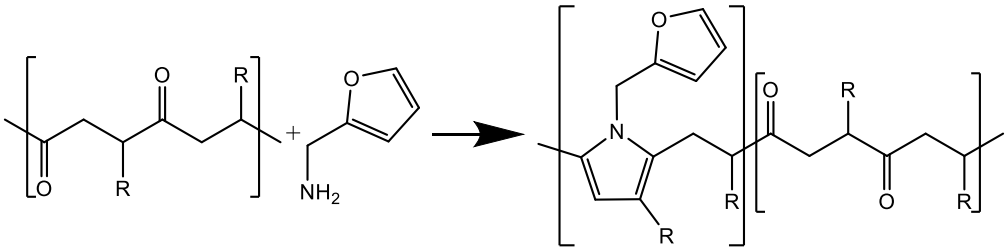

Figure 2. Paal-Knorr reaction of alternating aliphatic polyketone with furfurylamine [24]

This reaction pathway is advantageous because it can be carried out under relatively mild conditions (100 °C) and fast reaction kinetics (typically 4 hours) without requiring any catalyst while still providing high yield, typically 100% for the amine and up to 80%, for statistical reasons for the carbonyl. Notably, the reaction only produces water as by-product [17]. This process became the basis of other researches involving the functionalization of polyketone in the University of Groningen [17-19,24,26-33] and indeed, this project itself uses similar process to carry out polyketone functionalization, which will be described later.

The attempt for the chemical modification of polyketone with furan amino-subtituted compounds was originally done to prepare thermoset polymer networks which are able to undergo reversible reactions via Diels-Alder (DA)/retro-DA reactions [18] (Figure 3).

The furan groups grafted on the polyketone chain allows the formation of three-dimensional network structures after cross-linked with bismaleimide. Further research also discovered that the properties of the resulting material can be tuned by changing the crosslink density [24].

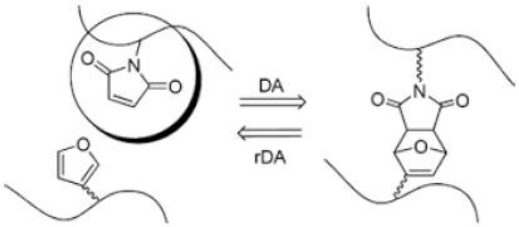

Figure 3. Schematic representation of Diels-Alder and reverse Diels-Alder reaction on furan and maleimide moiety [25].

The Diels-Alder reaction can form adducts with two different conformation: the endo and exo type (Figure 4). Endo conformation is a kinetic product from the reaction and is less stable compared to exo conformation, which is the desired result from the reaction. A special feature of the exo conformation is its ability to undergo reverse reaction upon heating, which in this case is commonly referred to as reverse/retro Diels-Alder reaction.

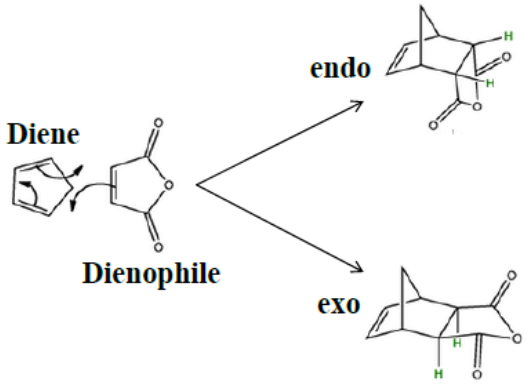

Figure 4. Schematic representation of Diels-Alder cycloaddition between cyclopentadiene and maleic anhydride showing the two possible conformations of the result [26].

Changing the crosslinking density in thermoset systems allows for fine-tuning of the system thermo-mechanical properties. Systems with high crosslink density typically display high hardness and modulus, while being remarkably resistant to solvents. Those properties come at the cost of poor elongation, low impact strength, low toughness and high brittleness [24]. On the other hand, a low cross-linked polymer system behaves as a flexible material [26]. The challenge in fine-tuning the crosslink density lies in finding a middle point where all the desired mechanical properties are at the acceptable level for a given application (Figure 5).

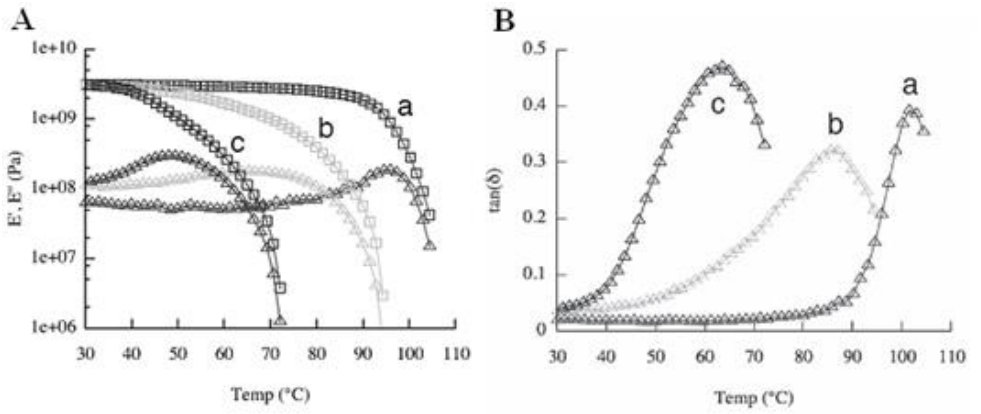

Figure 5. Loss (Δ) and storage (□) modulus behaviour in DMTA cycles for Polyketone with 50% furan functionalization (A) at different crosslink densities: (a) 1:1, (b) 1:0.5 and (c) 1:0.25 molar ratios between furan and bismaleimide. The softening point, taken as tan (δ) of the respective samples is displayed in (B) [24].

1.3 Composite Material

Composite material refers to materials which contain more than one component, each with different properties, but still visibly separate in the resulting material [34]. Composite materials can be manmade or natural formed materials. Wood is a common example of composite materials: it is formed of long fibres of cellulose which are held together by lignin [35]. On their own, lignin and cellulose have no significant structural strength but when combined, they form a much stronger material. One of the first utilization of composite by humans reflects that effect very clearly: early artificial composites are prized for their strength and durability, such as a combination of mud and straw, plywood, rammed earth, and concrete [36]. Straw bricks have been used as building material since the ancient times, and it currently remains in use when cheap, easily-manufactured building materials are desired (Figure 6).

Figure 6. Straw brick production in recent time near the Danube Delta [37].

In general, composite materials require having at least two components: the matrix and reinforcement. Based on the different type of matrices, modern manmade composites can be classified into four major categories: polymer matrix composite (PMC) (Figure 7), metal matrix composite (MMC), ceramic matrix composite (CMC) and carbon matrix composite or carbon-carbon composites [38]. The advantage of PMC compared to metal or ceramic-based composites is that the processability occurs at much lower temperatures. Like its matrix counterpart, PMC can be divided into two more classes: thermoset and thermoplastic composites. Thermoset resins are generally stronger due to the presence of crosslinks between the polymer chains, a feature that allows for applications at high temperature at the cost of being more brittle when compared to thermoplastics [39].

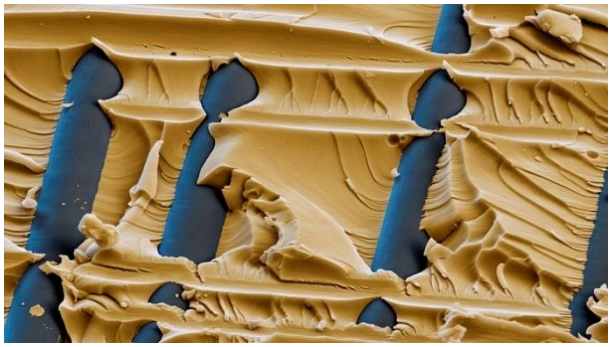

Figure 7. Microscopic image of carbon fibre-reinforced Baxxodur® epoxy resin system [40]

Knowledge about composite materials can lead to the development of materials that can be tailored for very specific purpose by using appropriate matrix/reinforcement combination and processing methods. Currently, composite materials are used in a wide variety of applications aside from the aforementioned structural applications: energy storage [41], membranous material [42,43], environmental clean-up [44], biomedical materials [45,46], optoelectronics [47], chemical catalysis [48], among other variety of fields and applications.

Another factor that affects the nature of composites is the interface interaction between matrix and reinforcement: a composite strength does not only depend on the choice of materials, but also how well the components bond to each other. In the case of polymer composite with fibre reinforcement, there are several possibilities of the interaction: selective adsorption of matrix components, conformational effects, penetration of polymer molecules into the fibre surface, diffusion of low molecular weight components from the fibre, and catalytic effects of the fibre surface on resin curing [49,50].

With respect to self-healing materials, polymer composites that are capable of autonomous self-healing have been described back in 1993, where healing was accomplished by incorporating hollow repair fibres filled with healing agent which releases their content as soon as microscopic cracks appear next to the fibre. As the crack ruptures embedded fibres, healing agents are released into the crack which is followed by rebonding of the damaged interfaces, closing the crack [51]. Further improvement on this concept was explored in 2001, where the fibres were replaced with microcapsules impregnated with a healing agent which forms a new polymer when coming into contact with a catalyst dispersed throughout the polymer matrix [52]. This approach allowed the material to reach 80% toughness recovery when the healing takes place at 80 °C [53].

1.3.1 Nanocomposite

It can be argued that the Ancient Mesoamerican culture was the first to utilize nanocomposites: the pigment known as Maya Blue was a mixture between dyes derived from *Indigofera suffruticosa* leaves mixed with palygorskite clay and other mineral additives [54]. Maya Blue pigment is able to withstand hundreds of years' worth of hot and humid condition which would have damaged other type of pigments. This is explained by a model where indigo dye fills the grooves present at the surface of palygorskite clay, forming a hydrogen-bonded organic/inorganic complex [54].

Since the 1980s, the industrial application of nanocomposites have been intensely investigated due to the available technology having reached the ceiling of traditional micrometer-scale composites when it comes to properties optimization, since the achievement of one of the required property involves the loss of another [55].The most significant benefit of lowering the scale of reinforcement components is that it allows more exact control over the orientation and interaction with the matrix,

allowing an even greater extent of control over the composite properties [38,56]. Thermoset nanocomposites have been the subject of many researches throughout the years since their advantage over conventional fibre composites are tremendous: the addition of up a single-digit percentage of reinforcing material is enough to increase the composite toughness by a factor of a thousand compared to the unadulterated matrix [38]. On the other hand, conventional composites require between 10%, up to 50% reinforcement to impart the desired mechanical and thermal properties [57]. A natural example of nanocomposite can be found as nacre (Figure 8), a material which is found as lustrous layer inside the shell of certain species of molluscs [58].

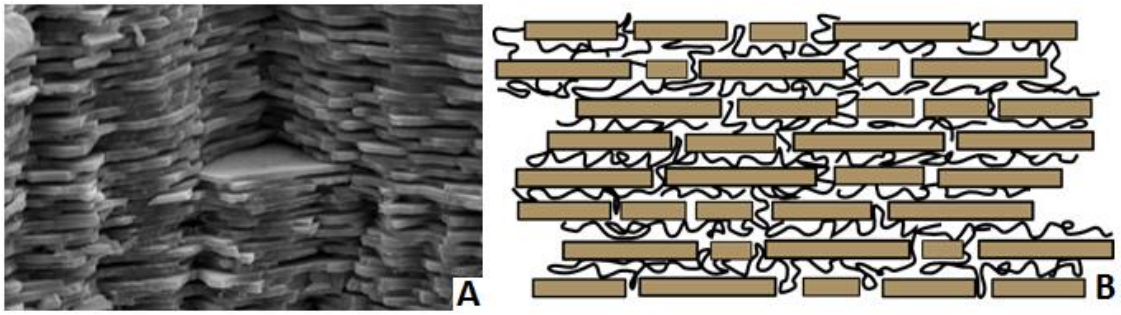

Figure 8. (A) Electron microscopy image of a fractured surface of nacre [59] and (B) Schematic of the microscopic structure of nacre layers [60]. Nacre is made from aragonite ($CaCO_3$) chips forming the matrix with biopolymer reinforcements sandwiched between them.

Nanocomposite can be classified into several classes based on its matrix component: ceramic-matrix nanocomposites typically utilize metal as their reinforcement, while metal-matrix nanocomposites have seen increasing number of carbon nanotube application as the reinforcement [61]. Finally, polymer-matrix nanocomposites (often shortened as polymer nanocomposites) utilize quite a varied types of material as filler and owing to their adaptable nature, have been used in a wide variety of application ranging from bone tissues engineering [62], flame retardants [63], drug delivery system [30], to 'standard' mechanical properties improvements [64], and many more [65].

1.4 Interpenetrating Polymer Network

By definition, interpenetrating polymer network (IPN) is a polymer comprising two or more networks. The polymer chains are at least partially interlaced at molecular level but not covalently bonded to each other (Figure 9) so that they cannot be separated unless the physical bonds are broken. In addition, and by definition, the components cannot be a mix of two preformed polymers [66]. A parallel between block copolymers and IPNs can be drawn based on how the length of their block or cross-link level affects the domain of each type of polymer [67]. The network may appear continuous at macroscopic scale, but are actually formed of two separate phases. Ideally, both polymers should be present as co-continuous, interlocking networks – which are also known as catenanes [67].

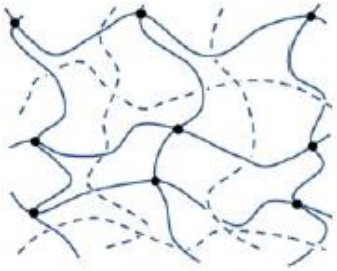

Figure 9. Interpenetrating polymer network: notice how the two polymer networks are not bonded to one another [68].

Due to its ability to retain large amounts of water and other biological fluids, IPNs have been a subject of researches for biomedical applications [69]. Common materials for IPN hydrogels are polysaccharides (e.g. alginate, starch, etc.) and proteins. Biomedical applications for IPN hydrogels have been widely explored and discussed elsewhere, however they will not be a part of this thesis.

IPN preparation can be divided into 3 general methods: 1) by mixing two monomers followed by crosslinking and polymerization (which can occur separately or simultaneously on both monomers); 2) dissolving a monomer in a polymer network followed by polymerization of the monomer; or 3) by blending two thermodynamically miscible polymers followed by crosslinking [68].

There are several types of IPN classification based on how the polymers bond to one another. Full IPNs refer to the state where both components are present as cross-linked networks, although there is negligible bonding between the two polymers [67]. Semi IPNs on the other hand, only have a single polymer network present in the system, enhancing its miscibility compared to full IPNs due to the relative freedom of movement of the non-crosslinked polymer [70].

The introduction of additional network to a polymer has been observed to improve the mechanical properties of the resulting mixture [68,70], but the effect is generally limited to a certain limit after the mechanical properties are observed to be worse than the original material (Figure 10). In this way, IPN is quite analogous to composite material, in which similar effect is encountered.

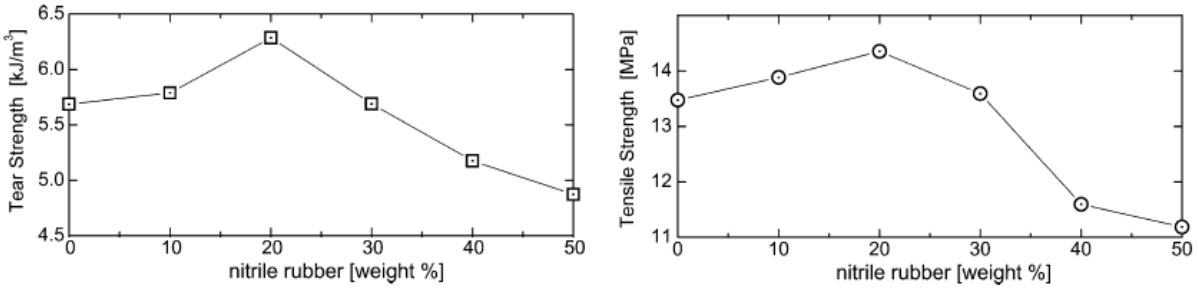

Figure 10. Strength properties of IPNs based on networks of nitrile rubber and a fluoropolymer [71].

Semi IPNs' morphology has attracted researches into developing it for mechanical actuators, as the actuation strength and breakdown strength is improved compared to the neat polymers [72]. Another application of semi IPNs that are of interest to this project is the application for self-healing polymers. The healing, in semi IPNs systems, occurs when cracks are bridged by the diffusion of non-cross-linked chains, with the cross linked component providing structural integrity. [70].

1.5 Self-healing Polymeric Materials

Self-healing materials are materials that are able to undergo partial or complete repair of recovery of their mechanical properties in a damage event [73]. Self-healing polymers are expected to have intrinsic capability to recover their load transferring ability after a damage that has been caused by external forces applied to the material. Such recovery can occur autonomously or be activated by an external stimulus (e.g. radiation), which is the case of non-autonomous self-healing [74]. The concept of self-healing polymeric materials has been put forth from as early as the 1980s, during the investigation of the welding and self-healing capability of poly(methyl methacrylate) (PMMA) and styrene-acrylonitrile (SAN) resin [75]. The research discovered that thermal healing in those two types of polymers can be achieved by subjecting the materials to temperature above their T_g, where physical links between molecular coils were established across the broken interfaces by interdiffusion [75]. The same research also found that vacuum drying of the sample and the reduction of the damaged surface area (by polishing) seem to reduce the speed of interdiffusion [75].

The strategy for self-healing material can be split into two general categories: extrinsic and intrinsic approach. Extrinsic approach refers to the use of foreign material (such as embedded healing agents) to achieve the material healing, while the intrinsic approach utilizes the material inherent properties stemming from specific chemical groups grafted to the polymer [26]. Both approaches have their own advantages and disadvantages: the main strength of extrinsic approachi s that the repair can take place in a completely autonomous fashion [52], while the disadvantage is directly related to its advantage: the external healing agent will start to deplete after each healing event, reducing the healing efficiency over time. On the other hand, the intrinsic self-healing approach tends to require external stimuli in form of mechanical, thermal, electrical, optical, or other form of stimuli such as pH changes or the presence of redox agents while theoretically able to carry out self-healing throughout the materials' lifetime [76].

Ideally, self-healing polymers are expected to be able to continuously repair and restore both their structural and mechanical properties over the duration of use [74]. Due to the huge number of properties that can be restored by self-healing materials, Wool and O'Connor developed a non-specific equation that can be used to describe the healing efficiency of different self-healing material systems [77]:

As mentioned in the Composite Material subchapter, the feasibility of developing a smart polymer matrix composite with the ability to repair cracks caused by thermal and mechanical loading has been investigated by impregnating hollow fibres with sealing chemicals and coating the surface of said fibres with polymers [50]. The resulting composite materials were found to have the ability to seal microcracks and repair damaged interfaces. The hollow fiber concept was further refined by dispersing catalyst and microcapsules containing a healing agent within the polymer matrix. In this system, healing is accomplished when crack ruptures the embedded microcapsules, releasing healing agent into the crack plane through capillary action (Figure 11). Polymerization of the healing agent is triggered by contact with the embedded catalyst, bonding the crack faces together [51].

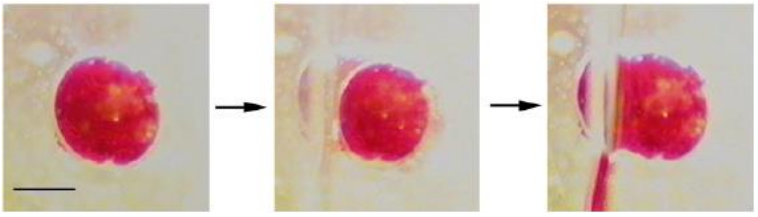

Figure 11. Video sequence showing the rupture and self-healing process using a microcapsule impregnated with healing agent. Red dye was added for visualization. The elapsed time from the left to right image is 1/15 second. Scale bar, 0.25 mm [52].

While both thermoplastic and thermoset materials are able to exhibit self-healing capability with proper treatment and composition, thermoset may be a slight disadvantage in terms of self-healing due to the rigidity and thermal stability: they have minimum chain mobility, the material property that is widely utilized for self-repair in thermoplastics [73]. However, this apparent disadvantage can be circumvented simply by changing the approach to self-healing in thermosets.

The previously-mentioned papers utilized two of the more suitable method of self-healing for thermosets: hollow-fiber impregnated with healing agent and microencapsulation [50,51]. Another approach that can be applied to self-healing thermoset materials is by using polymers with thermally-reversible cross-linkages [18,25,28,30-32,73]. In principle, using thermally-reversible cross-linkages could create self-healing materials that can be repaired infinite times, albeit with the trade-off of

requiring an external stimulus to initiate the healing process. Plaisted et al. [77], incorporated copper wire and coils into a polymer matrix, allowing the self-healing process to be triggered electrically. This approach shows that electrical self-healing can be applied using relatively simple manufacturing process.

For thermally-reversible and healable thermosets, one of the more widely-investigated crosslink strategy is the achieved through Diels-Alder (DA) reaction, which is capable of undergoing a reverse (rDA) reaction at sufficient temperature [18]. The reaction has been applied to the patent of cross-linked thermally reversible polymers in 1969, which claimed that the material was suitable for plastic replacement and adhesives [78]. Araya-Hermosilla et al. [31], reported successful self-healing capability of a polymer containing both reversible covalent (DA/rDA) and hydrogen bonding by modifying alternating aliphatic polyketone (PK) into new polymers containing furan and/or amine groups by using the Paal-Knorr reaction. The same research also suggested the possibility of using -OH containing moieties as hydrogen donors to avoid any unwanted side reaction occurring between amine groups and any unreacted carbonyl groups.

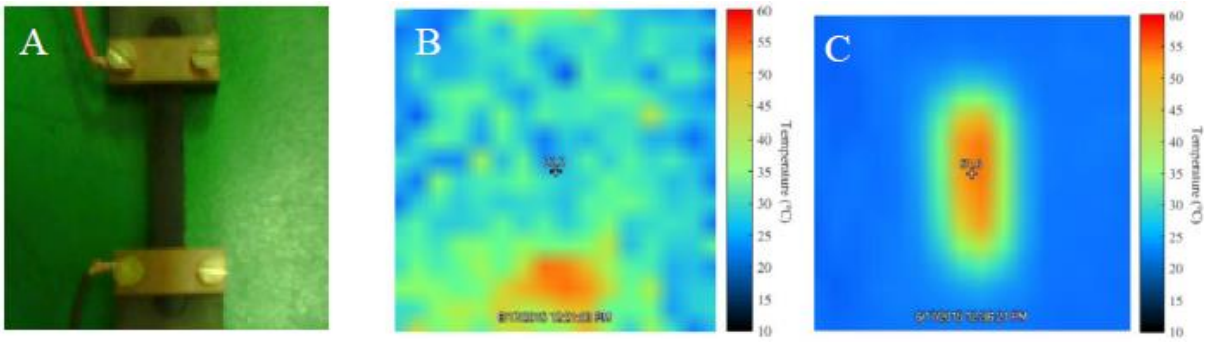

Figure 12. (A) Photograph of the polyketone-furan/bismaleimide/MWCNTs composite sample connected to the electrical circuit and its thermal images, (B) before and (C) during application of a voltage of 35 V [31].

The DA/rDA sequence has also been proven to work in a thermoset system that utilizes electricity as the stimulus for self-healing. In a similar vein with the work done by Plaisted and his group, Araya-Hermosilla, et al., introduced multiwalled carbon nanotubes (MWCNT) to act as both reinforcement and electricity-conducting network in a matrix composed of alternating aliphatic polyketone grafted with furan groups via Paal-Knorr reaction and cross-linked with bismaleimide [30]. The composite was prepared by a one-pot solvent-mix containing equimolar amount of polyketone functionalized with furan and bismaleimide (ratio 1:1 between furan and maleimide groups) and 5 wt. % of MWCNTs, resulting in an intrinsically self-healing thermoset/MWCNT nanocomposite capable of recovering structural damage by means of thermally reversible Diels-Alder links activated by electrical current. Thermal imaging in the referred work clearly indicates the conductivity of the sample, which in turn produces heat in form of resistive heating. The so-called Joule effect triggers the reconnection of decoupled DA adducts to recover the mechanical properties of the sample (Figure 12) [30].

Another approach that has been investigated for intrinsic self-healing is the use of interpenetrating polymer network (IPN), where the linear polymer was hypothesized to be able to assist with the self-healing process by diffusing into the microcracks [69]. The hypothesis was investigated with the conclusion that while the healing efficiency remains similar or slightly worse than polymer without added IPN, the addition of IPN in the polymer system increased the efficiency of subsequent healing processes compared to non-IPN [69].

1.6 Objective

Previous research on intrinsically self-healing polymer utilizing polyketone modified with furan and aminopropanol moiety has discovered that it is indeed possible to create a thermally reversible polymeric material that activates the self-healing mechanism through resistive heating, although said research did not systematically investigate the effect of different composition of the chemical moieties or crosslink density. Thus, this thesis will delve deeper into the characteristics of composites with different crosslink densities and ratios between polyketones containing furan or aminopropanol moieties.

The thesis aims to investigate the effect of utilizing a combination of reversible Diels-Alder and hydrogen bonds to create a non-autonomous self-healing polymeric material. Polyketone functionalized with furan groups will be reacted with bismaleimide to allow for Diels-Alder reaction to form crosslink networks. The formed Diels-Alder adducts allow for reversible opening/closing reaction and has been proven to facilitate the preparation of thermally reversible polymers.

The material will be reinforced with carbon nanotubes to improve the mechanical properties and allows the self-healing process to be triggered by electricity.

The thesis will be divided into two major parts; in the first part, functionalization of polyketone with furan will be carried out to create the material which will be used as matrix. The second part will deal with the characterization of the composite made by different compositions of polyketone-furan, polyketone-aminopropanol, bismaleimide and carbon nanotubes. Further investigation on the self-healing effect as a function of composition and electrical properties will be carried out.

2. Experimental Methods

2.1 Materials

The alternating aliphatic polyketone used has a total olefin content of 30 % of ethylene and 70 % of propylene (PK30, MW 2670 Da) [17,19,25,27]. Furfurylamine (Aldrich, ≥ 99 %) was distilled before used. 3-amino-1-propanol (Acros), multi-walled carbon nanotubes (Sigma-Aldrich, O.D. 10-15 nm; I.D. 2-6 nm; length 0.1-10 µm, >90% carbon)), (1,1-(methylenedi-4,1-phenylene) bis-maleimide (Sigma-Aldrich, 95 %), tetrahydrofuran (Boom B.V., analytical grade), chloroform ($CHCl_3$, Laboratory-Scan, 99.5 %), deuterated chloroform (Sigma-Aldrich 99.8 atom % D), toluene, and polyketone functionalized with 3-amino-1-propanol at 80% conversion (PK30AP80) were used as received.

2.2 Methods

2.2.1 Paal-Knorr Functionalization of Polyketone

Polyketone was prepared according to a previous research [14] and functionalized with furfurylamine via the Paal-Knorr reaction to act as the matrix for the composite [17]. All the resulting polyketones were given coded names according to the following convention: PK30 FU (from furfurylamine) ##, where ## refers to the percentage of moiety converted from the original polyketone group (Table 1).

Table 1. Composition of polyketones functionalized with furfurylamine group.

No.	Material	Conversion (%)	PK30 mass (g)	FU mass (g)
1	PK30FU20	20	20	2.9519
2	PK30FU40	40	20	5.9039
3	PK30FU60	60	20	8.8559
4	PK30FU80	80	20	11.8079

The polyketone functionalization process is based on the procedure that has been previously developed [17]. 20 g of polyketone was prepared in a 250 ml glass reactor equipped with an U type impeller and heated using an oil bath at 110 °C to allow the polyketone to liquefy. Once the temperature was reached, the stirrer was activated at 600 rpm. Furfurylamine were added dropwise in the first 20 minutes of the stirring, and the reaction was left to take place for 4 hours. The resulting products were then allowed to cool to room temperature before being doused with liquid nitrogen and pulverized with a mortar and pestle, producing a functionalized polyketone powder except for PK30FU20, which remained as a very viscous liquid. The ground polymer powder were then washed using Milli-Q water by stirring it for 15 minutes, repeated 3 times in order to remove any leftover amine compounds.

After filtering, the materials were freeze-dried for 72 hours, resulting in a powder in different shades of orange-brown color, which depended on the degree of conversion and material used.

2.2.2 Diels-Alder reaction and Interpenetrating Polymer Network preparation

Polymers grafted with furan groups were reacted with bismaleimide at an equimolar amount with the furan groups and mixed with different amounts of PK30AP80 using chloroform as solvent (with the polymer mixture's weight set to be 10% of the amount of solvent used). Additionally, multi-walled carbon nanotubes were added at 5% of the polymer mixture's weight to improve the material's mechanical modulus and facilitate electrical conduction [31].

All components were mixed inside a round-bottom flask and dissolved in chloroform which comprised of roughly 90% of the mixture's total mass (Table 2) and sonicated for 30 minutes. After sonication, the mixtures were then stirred for 24 h at 350 RPM in an oil bath set at 50 °C.

Table 2. Composition of various samples used in the experiment.

No.	Code	PK30 FU## %	PK30 AP80 %	PK30 FU## Mass (g)	PK30 AP80 Mass (g)	BMa Mass (g)	CNT Mass (g)
1	PK30FU80AP80 – A1	90	10	1.6	0.1778	1.2714	0.1516
2	PK30FU80AP80 – A2	50	50	1.1	1.1	0.8741	0.1537
3	PK30FU60AP80 – B1	90	10	1.7	0.1889	1.0120	0.1451
4	PK30FU60AP80 – B2	50	50	1.1	1.1	0.6548	0.1427
5	PK30FU40AP80 – C1	90	10	2.0	0.2222	0.7946	0.1508
6	PK30FU40AP80 – C2	50	50	1.25	1.25	0.4967	0.1498
7	PK30FU20AP80 – D1	90	10	2.3	0.2556	0.4569	0.1506
8	PK30FU20AP80 – D2	50	50	1.35	1.35	0.2682	0.1484

Afterwards, the resulting mixtures were dried in a vacuum oven at 50 °C for 24 hours. The resulting products were doused with liquid nitrogen to induce brittleness and ground with mortar and pestle.

2.2.3 Bar preparation

500 mg of the powder acquired from the Diels-Alder reaction were weighed and poured into a stainless steel mold lined with Teflon paper. The powders were then pressed using Schwabentan Polystat 100T with its operating condition set to 150 °C, 40 bar pressure for 30 minutes to form rectangular bars with rounded ends, with dimensions of 54 mm x 6 mm x 1 mm. The bars were allowed to cool down to room temperature and stored for further testing.

2.2.4 Characterization

The elemental analysis of the polymer samples was done using Euro EA elemental analyzer. ^{1}H NMR analysis was carried out using Varian Mercury 400 MHz Spectrometer with deuterated chloroform as solvent. ATR-FTIR spectra were recorded using Nicolet iS10 FT-IR spectrometer and analyzed with the Thermo Fisher OMNIC software. GPC measurements were done by dissolving the sample in THF spiked with toluene at a concentration of 1 mg/ml. The prepared samples were then analyzed using Hewlett Packard Series 1100 with elution rate of 1 ml/min at 40 °C. Polystyrene was used as standard and the software used to analyze the data was PSS WinGPC UniChrom. TGA analysis was done using Mettler Toledo TGA/SDT851 with nitrogen as inert gas, at temperature range of 20 to 700 °C, with heating rate of 10 °C/minute. TGA data analysis was done using STARe Evaluation Software. DSC analysis was done using Perkin Elmer DSC 7 with nitrogen as inert gas. Around 10-15 mg of the polymer samples were weighed and sealed inside aluminum pan. The samples were then subjected to temperature cycles where they were heated from 20 to 180 °C at a heating rate of 10 °C/minute before being cooled back to 20 °C for 3 times: first cycle was carried out to erase the material's thermal history, and the data used was from the second and third cycle. Electrical resistance test was carried out by clamping one piece of the bar between two copper electrodes and measuring the resistivity on the samples.

2.2.5 Healing Test

The healing process was done by thermal and electrical method. The thermal healing experiment involves reattaching broken bars by matching the broken pieces with each other, inserting them into the mold used in the original bar preparation method followed by pressing under the same

conditions: 150 °C, 40 bar pressure for 30 minutes of pressing. Similar attempts to re-attach broken bars were also carried out with the bars held by copper clamps on an aluminum rail, ensuring good contact between the broken pieces. The second thermal healing tests performed, involves scratching the surface of the bar pieces with a scalpel followed by heating using oven set to 150 °C and electrical current to start the rDA reaction. Afterwards, the scratched pieces were observed under microscope and checked for the presence of the original scratch.

2.2.6 Reworkability Test

Some of the bars that has been tested were broken, doused with liquid nitrogen, and ground into powder. From this powder, similar procedures to the bar preparation and characterization were performed to analyze the effect of the processes had on the chemical composition of the material.

3. Results and Discussion

3.1 Paal-Knorr Functionalization of Polyketone

The Paal-Knorr reaction between polyketone and amine compounds was carried out according to the reported procedure [17,31] at different molar ratios between the polyketone and furfurylamine with the maximum conversion target of 80% for the carbonyl groups as reported in literature [18]. The result of polyketone functionalization is listed in Table 3.

Table 3. Results of polyketone modification with furfurylamine. Expected C%, N% and XCO_{The} were based on reported literatures [26,28]. XCO_{Obs} was acquired based on the observed and expected C%. Mn, Mw, and Đ-value were acquired from GPC characterization.

No.	Polyketone	Elemental Analysis				X_{CO}^{The} (%)	X_{CO}^{Obs} (%)	η (%)	M_n (10^3)	M_w (10^3)	Đ
		Observed		Expected							
		C%	N%	C%	N%						
1	PK30FU80	72.90	5.82	75.79	6.21	80	77	96	3.05	6.44	2.1
2	PK30FU60	71.02	4.91	74.17	4.99	60	57	96	3.25	6.95	2.1
3	PK30FU40	56.66	4.34	72.29	3.59	40	31	78	3.27	7.52	2.3
4	PK30FU20	64.37	1.88	70.09	1.95	20	18	92	3.48	8.69	2.5

The relatively high conversion efficiency is a proof on the high yield produced by the Paal-Knorr reaction. The efficiency observed during this project was similar with the previous research utilizing similar process [17,26,28], indicating a successful functionalization across the samples except for the lower efficiency for PK30FU40. The cause of the lower conversion efficiency was not immediately clear, but possibly caused by a long period between furfurylamine distillation and functionalization reaction [31].

^{1}H NMR analysis (Figure 13) suggests that the Paal-Knorr reaction has managed to attach furfurylamine to the polyketone. Peak (1) at 5.6 ppm indicates the presence of pyrrole ring, while (2) at 4.9 ppm represents the $-CH_2$ group attached between pyrrole and furan groups. (3), (4), and (5) at roughly 6, 6.25 and 7.16 ppm corresponds with the protons contained within the furan group attached to the pyrrole ring [17]. Unfortunately, the solvent used for the ^{1}H NMR ($CDCl_3$) also gives signal at 7.16 ppm, skewing the intensity of the resulting signal.

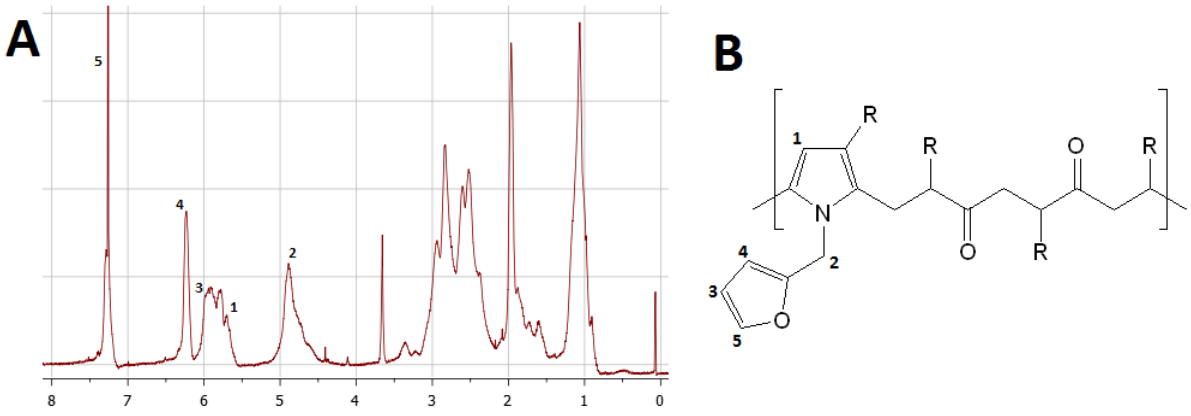

Figure 13. (A) ^{1}H NMR spectra of polyketone functionalized with furfurylamine at 80% conversion (PK30FU80). (B) The chemical structure of polyketone with furan group attached. Both (A) and (B) have numerical annotation which relates the signal with its respective structure.

The NMR analysis is further supported by results from ATR-FTIR analysis of the same sample (Figure 14). Signals from pyrrole ring appeared at 3114 cm^{-1} and 1597 cm^{-1}, while the attached furan

groups were detected at 3150 cm^{-1} and 737 cm^{-1} [78]. Across all the polyketone functionalized with furfurylamine, the previously-mentioned signals consistently appear, albeit at different intensity (see Appendix A for the rest of the characterization). This suggests that the functionalization process has indeed been successfully carried out.

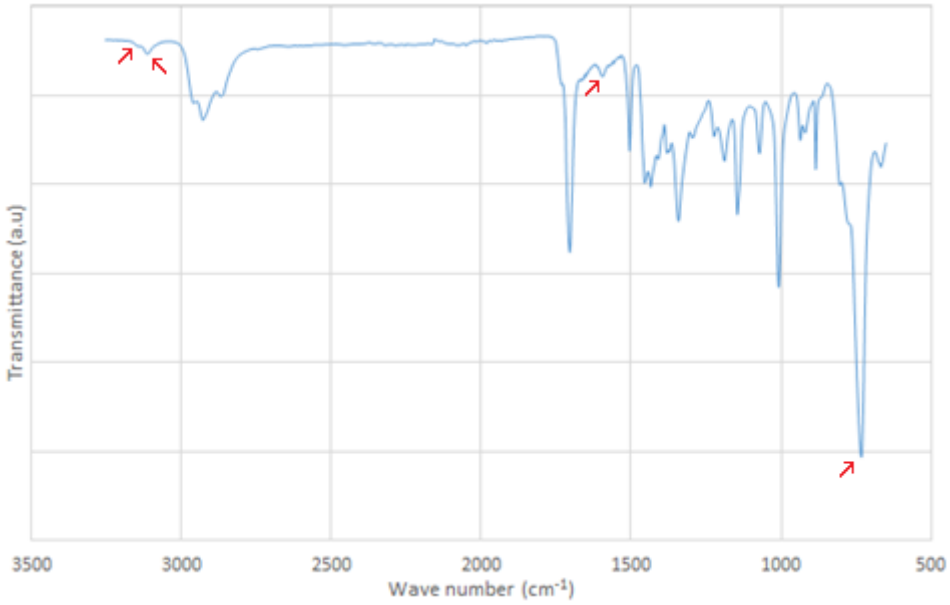

Figure 14. ATR-FTIR spectra of polyketone functionalized with furfurylamine at 80% conversion (PK30FU80).

3.2 Diels-Alder Reaction and Interpenetrating Polymer Network Preparation

Once the characterization of functionalized polyketone has been completed, the samples were reacted with bismaleimide and combined with PK30AP80 using chloroform as solvent for 24 hours at 50 °C to create the desired composite polymer. Again, after the process has been carried out, the sample was characterized with ATR-FTIR to monitor for the DA cycloaddition [78], and DSC to look into the samples' thermal reversibility (and by extension, its recyclability).

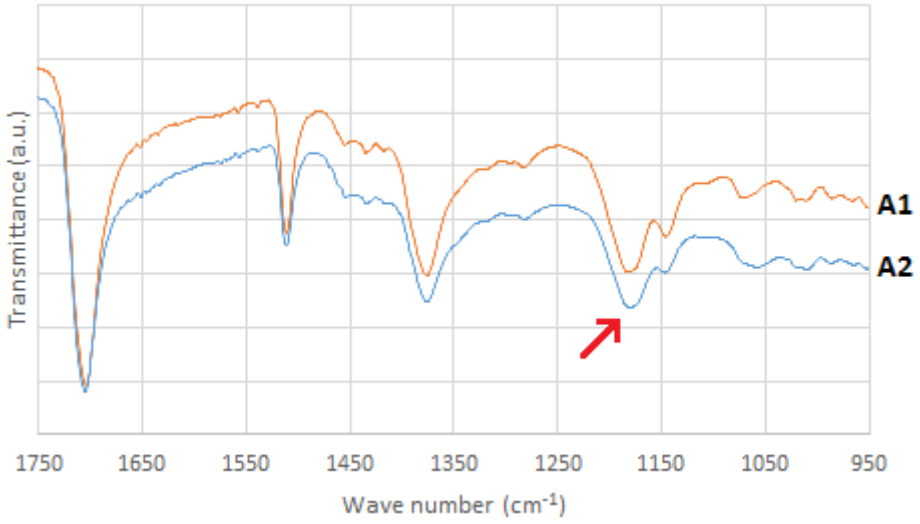

Figure 15. ATR-FTIR spectra of PK30FU80AP80 with different ratio between PK30FU80 and PK30AP80: A1 (90% PK30FU80, 10% PK30AP80) and A2 (50% PK30FU80, 50%PK30AP80).

The presence of a spectral band of C-N-C DA adduct at 1185 cm^{-1} confirms that there is Diels-Alder cycloaddition in the finished product [31]. As can be seen from the spectra (Figure 15), the relative height of the C-O stretch corresponds to the amount of DA bond formed between furan and

maleimide groups [26]. Unlike in the previous works, the molar ratio between furan and bismaleimide in this research is not systematically changed; they remain at 1:1. Only the amount of furan group attached to the polyketone backbone and also the ratio between PK30FU## and PK30AP80 are changed, as outlined in the experimental section.

Thermal behaviour of all the samples were also analyzed using TGA and DSC. TGA analysis was done using nitrogen as inert gas, at temperature range of 20 to 700 °C, with heating rate of 10 °C/minute (Figure 16).

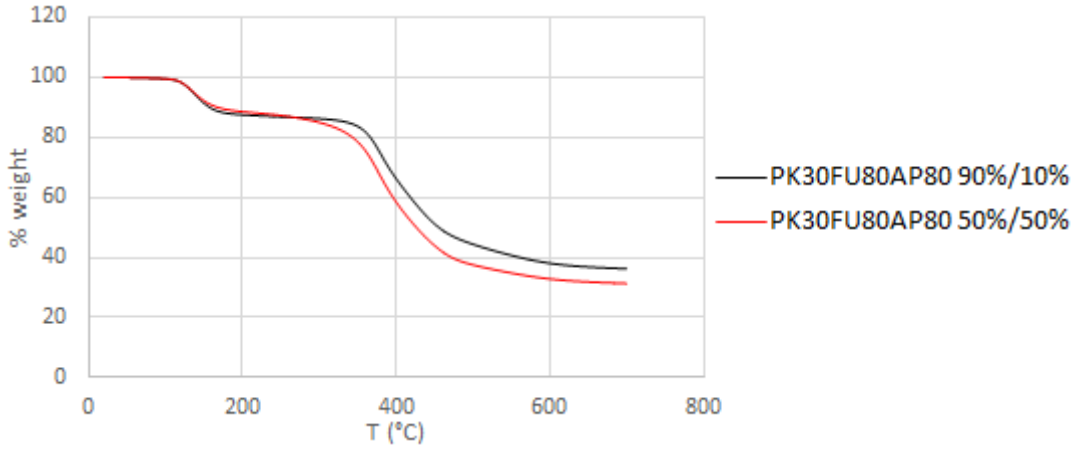

Figure 16. TGA thermogram of crosslinked polyketone composites A1 and A2.

The TGA result shows more relevant degradation of the sample containing lower degree of furan group, reinforcing the idea that furan groups can be attached to the surface of carbon nanotubes [26]. The degradation of both samples itself starts at around 100 °C, most likely caused by the presence of residual water.

DSC tests were done by subjecting the samples into three thermal cycles from 20 to 180 °C, at the heating rate of 10 °C/minute. As the first cycle's was meant to erase the material's thermal history acquired by preparation [26], only the data from second (labeled Cycle 1) and third cycle (labeled as Cycle 2) will be presented (Figure 17).

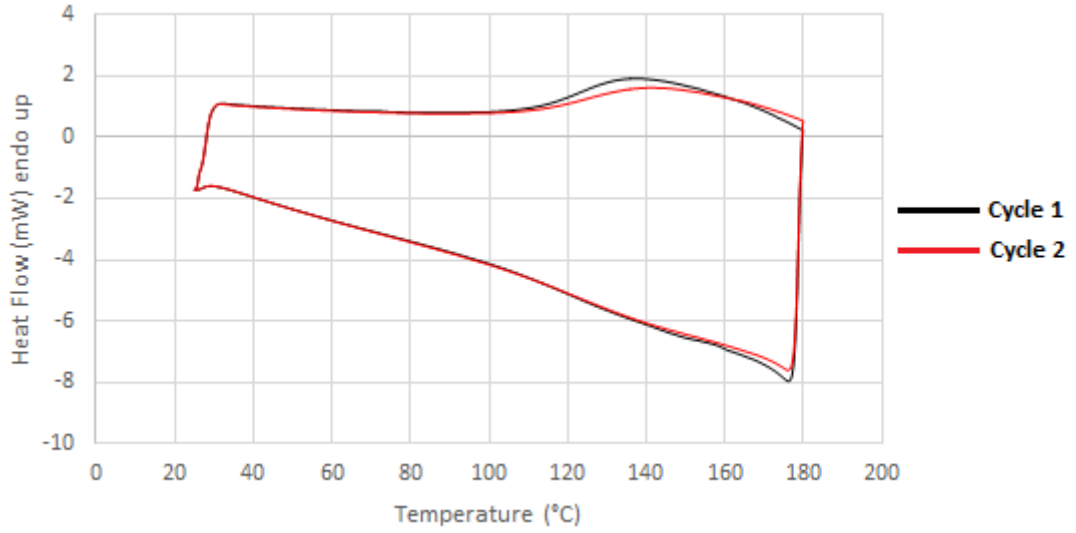

Figure 17. DSC thermogram of crosslinked sample A1 (PK30FU80AP80, 90%/10% composition).

The instantly noticeable fact is that both cycles are very similar to each other, with slightly different peak at starting at around 110 °C to 180 °C. This indicates a very good thermal reversibility of the sample, although the slight difference in the peak shows that it is not 100% reversible. There are some possible explanations: some of the material was suspected to undergo aromatization, reducing the amount of reversible bonds present when it is subjected to a sufficient temperature [26]. Another possible cause of the changes was the formation of the unstable endo conformation of the Diels-Alder adduct as opposed to the desired exo conformation, which are stable and can undergo reverse Diels-Alder reaction when heated [26].

The enthalpy required to carry out the reverse-DA reaction can be correlated with the amount of DA adduct present in the system. To confirm this, the area under the curve was calculated and normalized with the amount of PK30FU## (Figure 18), as PK30AP80 is not seen to facilitate crosslinking and would not have contributed to the enthalpy of the Diels-Alder reaction. Only the curves from sample A1's two cycles are shown here for brevity.

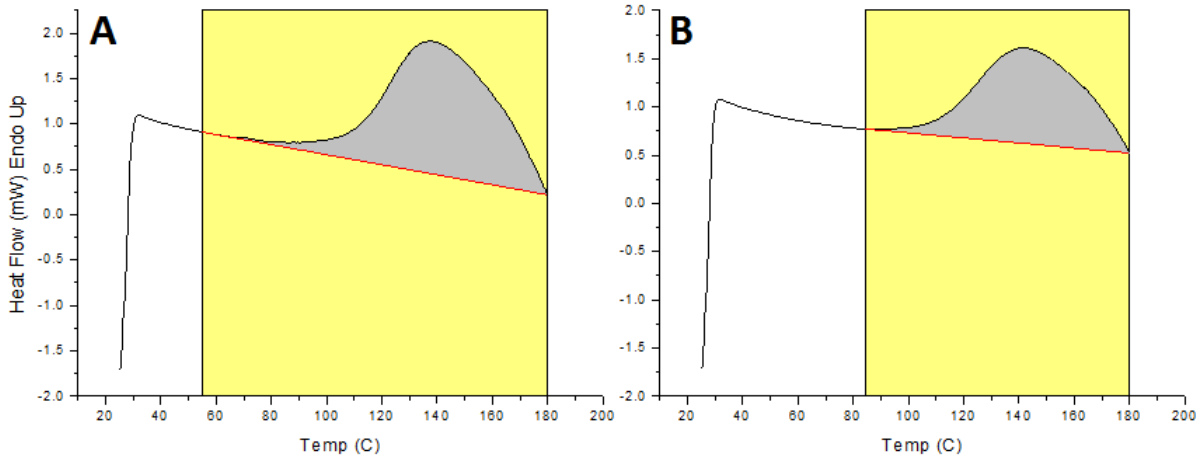

Figure 18. Area calculation to determine the effect of PK30AP80 on the enthalpy of Diels-Alder reaction within the system. Only sample from A1 was shown during the first (A) and second (B) heating cycle.

The enthalpy calculation showed an average of 13.70 J/g FU on the first cycle, which decreased to 7.95 J/g FU on the second cycle, a 44% decrease compared to the first thermal cycle. Again, this opens the possibility that some of the DA bond undergoing aromatization which reduces the number of bonds that can undergo the DA-rDA reaction, or that the resulting DA bond forms an endo instead of exo conformation and disrupting the reverse Diels-Alder reaction.

In order to confirm the composites' conductivity and their ability to convert electricity into heat (also known as resistive heating), the bars were clamped on each end to a copper clamp and had current set to run through them. An infrared camera was then used to check each bar's temperature (Figure 19).

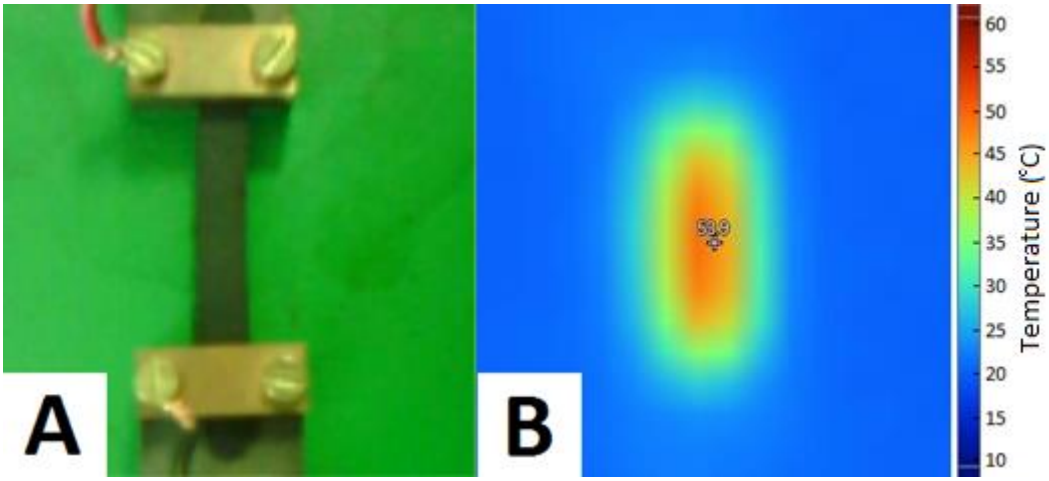

Figure 19. (A) Photograph of the bar set up to conduct electricity, (B) thermal image of the bar with electrical current running at V = 30 volt.

Previous research has managed to induce self-healing in a similar system by keeping a current supplied by 35 volt overnight, which results in a redistribution of MWCNT aggregates as confirmed by SEM [26].

Each bars' resistivity were measured to find the correlation between the composition of the bar and the effect it has on electrical properties. It was postulated that higher furan content will lead to better conductivity in the sample, as the previous report has stated that furan is able to attach to MWCNT by forming crosslinks [26] which in turn allow for a more even distribution of MWCNT throughout the sample, allowing it to have better electrical conductivity. It was found that for both ratios of PK30FU ## to PK30AP80, higher presence of furan moiety does correspond to higher conductivity (or in the other way around: lower resistivity) of the sample (Figure 20).

The anomalous reading on PK30FU60 – PK30AP80 50%/50% composition on Figure 20.B could be attributed to the poor quality of the sample; at the time resistivity measurements were carried out, most of the samples from that particular composition has been used for self-healing tests which would have changed their morphology. Ignoring the value of that measurement, it can be seen that the other 3 values follow the same trend as its counterpart on the 90%/10% composition.

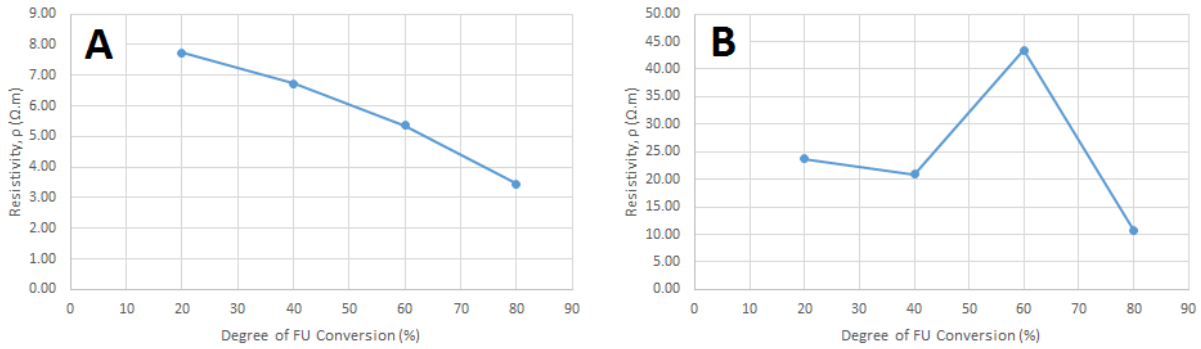

Figure 20. (A) Resistivity of electrical bar containing 90% PK30FU ## and 10% PK30AP80 based on the PK degree of conversion and (B) resistivity of electrical bar containing 50% PK30FU ## and 50% PK30AP80 based on the PK degree of conversion.

This result shows that there is an indirect correlation between dispersion of MWCNT and electrical resistivity. In the future, this could be a topic to be investigated further or even applied in experiments as a mean to create electrical sensor.

3.3 Healing Test

Previous studies have discovered that polyketone which has been functionalized using furfurylamine crosslinked wit bismaleimide, or 3-amino-1-propanol (or the combination of both in a single polyketone backbone) can exhibit self-healing when exposed to sufficient temperature [18,26]. The attempt to create a mixture containing two different polymer, is therefore, quite novel in this theme's context. The samples were broken and healing process were attempted using several different methods.

The first trial consists of assembling the broken pieces back into the mold followed by reapplying the initial processing condition of 150 °C and 40 bar of pressure for 30 minutes. This results in a mended bar which visually shows no sign of damage (Figure 21).

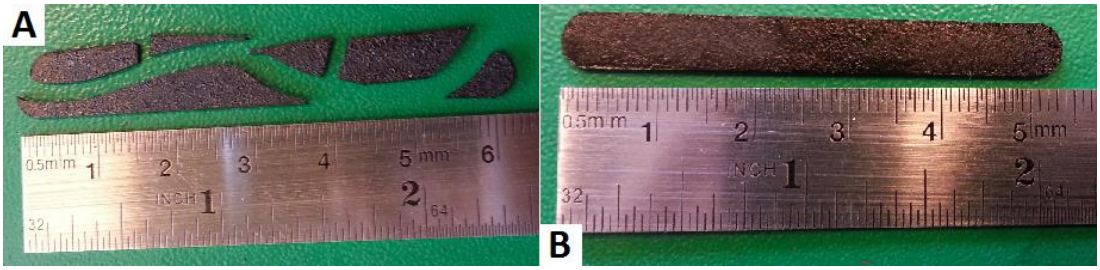

Figure 21. Broken bar of sample B1, which fell during processing. No picture of original sample is available. (A) Its shape before, and (B) after the healing process using Schwabentan Polystat 100T.

The bar re-welding tests were also conducted using electricity: each pieces of broken bars were clamped and matched, and pressed together using the aluminum rail. Roughly 50 volt of electricity were then flowed to achieve the temperature of 120 °C, in which the rDA reaction can begin to soften the bar, theoretically allowing for reptation of the polymer chains to begin as the starting point for the healing process. The attempt was met with failure however, as among all the 8 available samples, none managed to reattach the two sides where the breaking occurs. One possible explanation of the failure was the very low pressure applied to press the two faces together, preventing anything other than reptation at the surface of the cracked faces to take place between the gaps of the two bars, and causing interdiffusion of the polymer chains between the two faces not to occur.

Similar to the rewelding test, the scratch healing place was carried out using both heat and electricity. The bars' surface was scratched with a scalpel, and healed both oven set to 150 °C over a period of 24 hours, and with electrical current running through the sample with differing voltage to achieve a temperature of 120 °C where the rDA reaction is predicted to have already taken place albeit at a slower rate. Temperature of electrical healing was monitored using IR thermal camera. The self-healing efficiency was not quantitatively measured, and only evaluated visually with the assistance of an optical microscope at 200x magnification.

The thermal healing process (Figure 22) has shown that the material does heal minor surface damage, albeit with some residual damage still partially visible on the surface. Using pieces of bar broken from a failed tensile test evaluation, the notches from the clamp were also successfully removed (visible on the left hand side of picture Figure 22 (D) and (E)).

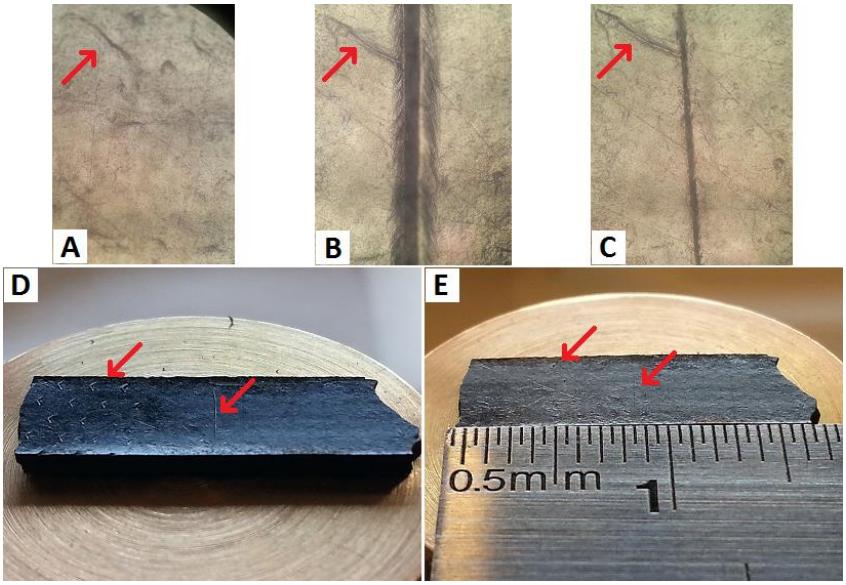

Figure 22. Microscopic image of the PK30FU20AP80 with 90%/10% composition (D1) bar at 200x magnification (A) before, (B) after damage, and (C) after subjected to 150 °C treatment in oven for 24 hours. Photograph of actual sample bar are given (D) with the damage visible, and (E) after the healing process. Red arrows were used to indicate points of interests.

The electrical surface healing tests were carried out using a similar setup seen in Figure 19 with a considerably shorter bar leftover from a failed tensile test, with surface damage introduced using a scalpel (Figure 23). The electrical healing test failed to produce any significant changes however, with no real repair taking place even when viewed at 200x magnification. This is at odds with the previous finding in which resistive heating were able to restore, even improve the mechanical properties of the bars [31].

One possible explanation was the work mentioned above used the healing process to repair internal damage which appear after the bars have been tested using DMTA, allowing for a much smaller cracks to occur within the structure as opposed to the surface scratches which are visible with naked eye [31]. Another plausible explanation is that a huge, centralized damage as in the case of surface scratches may simply require more time to heal compared to internal microcracks [77,79].

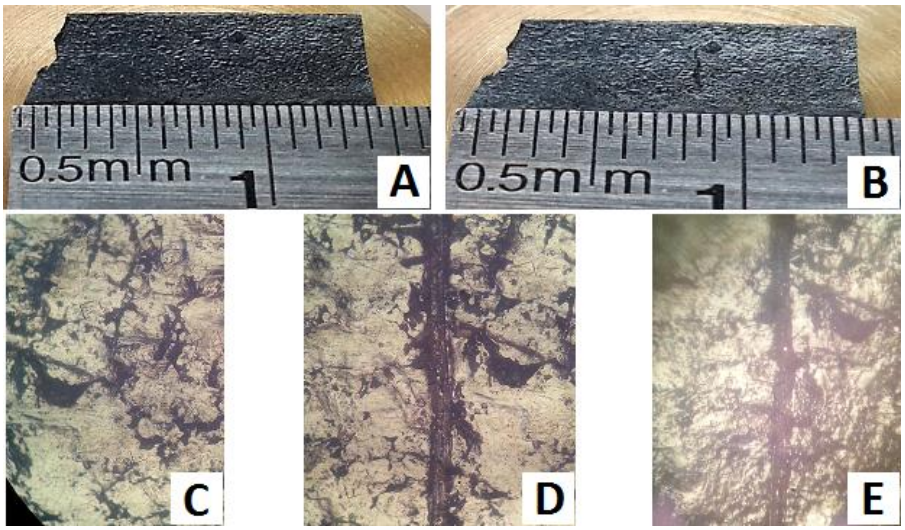

Figure 23. Photograph of PK30FU80AP80 with 90%/10% composition: (A) broken sample bar and (B) with the damage and after the electrical healing. Microscopic image of the bar at 200x magnification (A) before, (B) after damage, and (C) after subjected to 120 °C treatment from electrical current for 24 hours.

3.4 Reworkability Test

Similar to healing test, the reworkability test also investigates the composite's ability to reform into its original state after being destroyed by grinding. This is tied to the material's recyclability once the original product has outlived its usefulness.

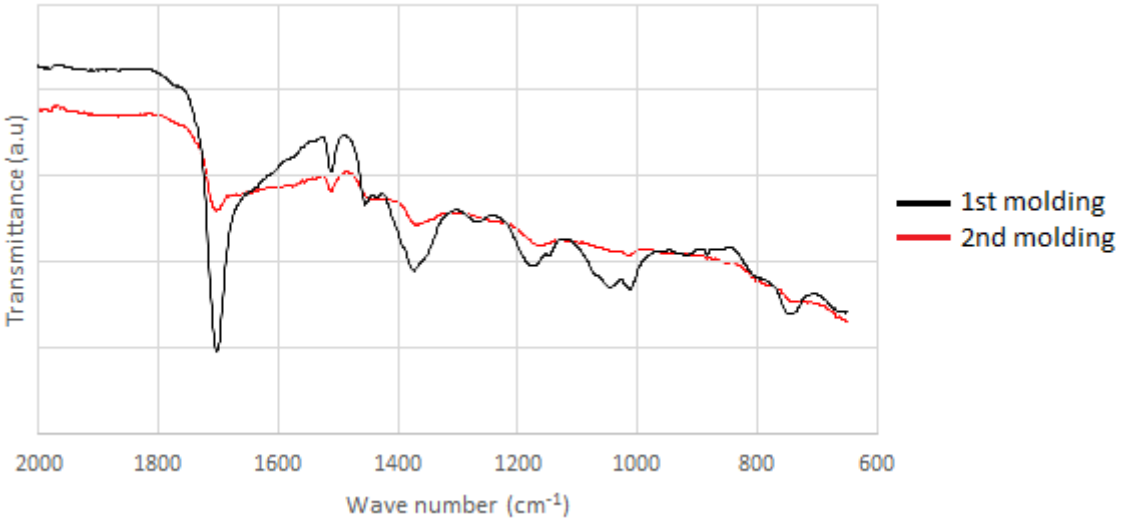

Figure 24. Comparison of ATR-FTIR spectra of PK30FU20AP80 50%/50% on the original and reworked bar. Several peaks that undergo notable change are: $V_s^{C=O}$ at 1707 cm^{-1}; $V_s^{C=C}$ 1507 cm^{-1}; V_s^{N-C} at 1345 cm^{-1}; and V_s^{C-N-C} at 1185 cm^{-1}.

In almost all the cases, the magnitude of the signals from reworked materials were lower from its original material (Figure 24); this may indicate a degradation of the original sample, results in a worse mechanical properties which would deem the material to have a low recyclability. At macroscopic level, all the materials show no significant visual differences between the samples before and after rework. However, without actual mechanical testing, the ATR-FTIR were only able to give indication, not a definite comparison that the material's mechanical properties are actually worse after being reworked.

4. Conclusion & Recommendations

In this project, we have managed to synthesize an intrinsically self-healing nanocomposite material utilizing a combination of Diels-Alder reversible reaction and hydrogen bonding to facilitate the self-healing, with multi-walled carbon nanotubes added as reinforcement to the mixture. The preparation of the material was followed by systematic investigation into the effect of different composition on the electrical and self-healing properties.

Characterization results from NMR, ATR-FTIR, elemental analysis and GPC have confirmed a successful incorporation of furan groups into a polyketone backbone at different conversion to ensure significant changes in the resulting composite.

ATR-FTIR analysis confirmed the presence of C-N-C Diels-Alder adduct, indicating a successful crosslinking reaction. TGA thermogram showed that samples which contain less furan group exhibit more degradation, indicating that polyketone functionalized with furan groups are able to be attached to MWCNT, resulting in an increased thermal stability. DSC analysis further confirms the thermally-reversible nature of the resulting polymer, as proven by the thermogram from the analysis which almost perfectly overlaps with each other across all samples.

Enthalpy calculation from the DSC thermogram shows that there is a reduction in enthalpy from one cycle to the next. The two possible causes would be that some of the material undergoing aromatization at higher temperature, or that the Diels-Alder adduct that formed / reformed were of the endo conformation, which is unstable as opposed to the stable and thermoreversible exo conformation.

The electrical property test also found that in most of the sample, the resistivity (ρ) of each composition is inversely correlated with the amount of polyketone functionalized with furan group. Furan group's ability to form crosslinks with MWCNT is suspected to be the cause of this behaviour [31]. Higher presence of furan group would allow the MWCNT to be dispersed better in the composite during mixing, leading to an overall better conductivity in the sample. This can lead to using resistivity measurement as an indirect way to measure the dispersion of MWCNT in a composite, something that could be useful for future research into similar topic.

Self-healing and reworkability tests both showed that the composite were able to be healed and reshaped into its original form using heat yet shows minor changes when the repair process was attempted using joule heating. One difficulty encountered during the self-healing test was the inability to induce uniform damage on all the samples. The material shows significant difference when analysed with ATR-FTIR, possibly caused by degradation of the material itself.

In the end, this thesis managed to systematically analyse the effect of different composition on the self-healing capability and electrical properties of a self-healing thermoset nanocomposites based on physical and thermally-reversible linkages. It was discovered that the composition affects the resistivity of the composite, likely caused by the difference in MWCNT dispersion in the composite material. This leads to the possibility of tailoring the material to have specific electrical resistivity based on its composition, for use as part of a sensor equipment or as a part of the electrical circuit itself.

In the future, a more thorough and systematic investigation into the mechanical properties would be an interesting research to look into. Another possible course of investigation would be to introduce different conductive material into the mixture such as metal fibres, in order to compare the cost and effectiveness of the resulting composite.

References

1. Labrude, P.; Becq, C. Le pharmacien et chimiste Henri Braconnot (Commercy 1780-Nancy 1855). pharm 2003, 91, 61-78.

2. Coran, A. Y. 7 - Vulcanization. In Science and Technology of Rubber (Third Edition); Mark, J. E., Erman, B. and Eirich, F. R., Eds.; Academic Press: Burlington, 2005; pp 321-366.

3. ACS Bakelite: The World's First Synthetic Plastic. http://www.acs.org/content/acs/en/education/whatischemistry/landmarks/bakelite.html (accessed October 9, 2015).

4. Freinkel, S. Plastic: A Toxic Love Story; Houghton Mifflin Harcourt: Boston, 2011; .

5. Lee, K. R. Wartime Rationing. In Editorial Research Reports 1942CQ Press: Washington, D.C., United States, 1942; Vol. I, pp 17-38.

6. MIT Inventing Modern America: Insight - Stephanie Kwolek. http://www.webcitation.org/5h0GDyhkl.

7. Glenn, F. E. Chloroprene Polymers. In Encyclopedia of Polymer Science and TechnologyWiley-Blackwell: Hoboken, 2002; .

8. Fried, J. R. Polymer Science and Technology; Prentice Hall: Upper Saddle River, 2014; .

9. Ophardt, C. Polymer Fundamentals. http://chemwiki.ucdavis.edu/Organic_Chemistry/Polymers/Polymer_Fundamentals.

10. Baeurle, S. A.; Hotta, A.; Gusev, A. A. On the glassy state of multiphase and pure polymer materials. Polymer 2006, 47, 6243-6253.

11. IUPAC IUPAC Gold Book - thermosetting polymer. http://goldbook.iupac.org/TT07168.html.

12. Ballauf, F. D.; Bayer, O. D. D. H. C.; Teichmann, L. D. Verfahren zur Herstellung von hoehermolekularen Additionsprodukten aus niederen Olefinen und Kohlenoxyd A process for preparing hoehermolekularen addition products of lower olefins and carbon monoxide. 1953.

13. Sen, A., Ed.; In Catalytic Synthesis of Alkene-Carbon Monoxide Copolymers and Cooligomers; Springer US: 2003; .

14. Drent, E.; Mul, W. P.; Smaardijk, A. A. Polyketones. In Wiley-Blackwell: 2001; .

15. Hasan, N. H. Synthesis of perfectly alternating carbon monoxide/olefin polyketones using a sulfonated diphosphine catalyst system. 2009.

16. Drent, E. Process for the preparation of polyketones. 1986.

17. Zhang, Y.; Broekhuis, A. A.; Stuart, M. C. A.; Picchioni, F. Polymeric amines by chemical modifications of alternating aliphatic polyketones. J Appl Polym Sci 2007, 107, 262-271.

18. Zhang, Y.; Broekhuis, A. A.; Picchioni, F. Thermally Self-Healing Polymeric Materials: The Next Step to Recycling Thermoset Polymers? Macromolecules 2009, 42, 1906-1912.

19. Hamarneh, A. I.; Heeres, H. J.; Broekhuis, A. A.; Sjollema, K. A.; Zhang, Y.; Picchioni, F. Use of soy proteins in polyketone-based wood adhesives. Int J Adhes Adhes 2010, 30, 626-635.

20. Reuter, P.; Fuhrmann, R.; Mücke, A.; Voegele, J.; Rieger, B.; Franke, R. -. CO/Alkene Copolymers as a Promising Class of Biocompatible Materials - Examination of the In Vitro Toxicity. Macromol.Biosci. 2003, 3, 123-130.

21. Pérez-Foullerat, D.; Hild, S.; Mücke, A.; Rieger, B. Synthesis and Properties of Poly(ketone-co-alcohol) Materials: Shape Memory Thermoplastic Elastomers by Control of the Glass Transition Process. Macromol.Chem.Phys. 2004, 205, 374-382.

22. Wong, P. K.; Pace, A. R.; Weber, R. C. Water soluble polyketones. 1999.

23. Wong, P. K. Polyamine with grafted vinyl polymers. 2001.

24. Toncelli, C.; De Reus, D. C.; Picchioni, F.; Broekhuis, A. A. Properties of Reversible Diels-Alder Furan/Maleimide Polymer Networks as Function of Crosslink Density. Macromol.Chem.Phys. 2012, 213, 157-165.

25. Sanyal, A. Diels–Alder Cycloaddition-Cycloreversion: A Powerful Combo in Materials Design. Macromolecular Chemistry and Physics 2010, 211, 1417-1425.

26. Araya-Hermosilla, R. Thermally reversible thermoset materials based on the chemical modification of alternating aliphatic polyketones. 2015.

27. Zhang, Y.; Broekhuis, A. A.; Stuart, M. C. A.; Fernandez Landaluce, T.; Fausti, D.; Rudolf, P.; Picchioni, F. Cross-Linking of Multiwalled Carbon Nanotubes with Polymeric Amines. Macromolecules 2008, 41, 6141-6146.

28. Toncelli, C. Functional Polymers from Alternating Aliphatic Polyketones - Synthesis and Applications. 2013.

29. Araya-Hermosilla, R.; Broekhuis, A. A.; Picchioni, F. Reversible polymer networks containing covalent and hydrogen bonding interactions. European Polymer Journal 2014, 50, 127-134.

30. Araya-Hermosilla, E.; Orellana, S. L.; Toncelli, C.; Picchioni, F.; Moreno-Villoslada, I. Novel polyketones with pendant imidazolium groups as nanodispersants of hydrophobic antibiotics
. Journal of Applied Polymer Science 2015, 132.

31. Araya-Hermosilla, R. Electrically responsive thermoset nanocomposite based on Diels-Alder chemistry. 2015.

32. Araya-Hermosilla, R. Intrinsic self-healing thermoset through covalent and hydrogen bonding interactions. 2015.

33. Araya-Hermosilla, R.; Fortunato, G.; Pucci, A.; Raffa, P.; Polgar, L.; Broekhuis, A. A.; Pourhossein, P.; Lima, G. M. R.; Beljaars, M.; Picchioni, F. Thermally reversible rubber-toughened thermoset networks via Diels–Alder chemistry. European Polymer Journal 2016, 74, 229-240.

34. RSC Composite materials.
http://www.rsc.org/Education/Teachers/Resources/Inspirational/resources/4.3.1.pdf.

35. AAS Putting it together – the science and technology of composite materials - Academy of Science.
http://www.sciencearchive.org.au/nova/059/059key.html.

36. Strong, B. History of Composite Materials - Opportunities and Necessities. 2002.

37. Soare Danube Delta: making Construction Material.
https://en.wikipedia.org/wiki/File:RomaniaDanubeDelta_MakingMaterialForCOnstructing0002jpg.JPG (accessed May 6, 2016).

38. Ratna, D. Handbook of Thermoset Resins; iSmithers: 2009; .

39. Dante, R. C.; Santamaría, D. A.; Gil, J. M. Crosslinking and thermal stability of thermosets based on novolak and melamine. J Appl Polym Sci 2009, 114, 4059-4065.

40. BASF Automotive Lightweight Composites. https://www.basf.com/en/company/research/our-focus/lightweight-composites.html.

41. Cao, X.; Tan, C.; Zhang, X.; Zhao, W.; Zhang, H. Solution-Processed Two-Dimensional Metal Dichalcogenide-Based Nanomaterials for Energy Storage and Conversion. Adv Mater 2016, n/a-n/a.

42. Dixita, S.; Palb, S. Recent Advanced Technologies in the Processing of Hybrid Reinforced Polymers for Applications of Membranes. Polymers & Polymer Composites 2016, 24, 289-305.

43. Li, D.; Yan, Y.; Wang, H. Recent advances in polymer and polymer composite membranes for reverse and forward osmosis processes. Progress in Polymer Science 2016.

44. Hernández-Hernández, K. A.; Illescas, J.; Díaz-Nava, M. d. C.; Muro-Urista, C. R.; Martínez-Gallegos, S.; Ortega-Aguilar, R. E. Polymer-Clay Nanocomposites and Composites: Structures, Characteristics, and their Applications in the Removal of Organic Compounds of Environmental Interest. Medicinal Chemistry 2016, 6.

45. Cramer, N. B.; Stansbury, J. W.; Bowman, C. N. Recent Advances and Developments in Composite Dental Restorative Materials. J. Dent. Res. 2010, 90, 402-416.

46. Scholz, M. -.; Blanchfield, J. P.; Bloom, L. D.; Coburn, B. H.; Elkington, M.; Fuller, J. D.; Gilbert, M. E.; Muflahi, S. A.; Pernice, M. F.; Rae, S. I.; Trevarthen, J. A.; White, S. C.; Weaver, P. M.; Bond, I. P. The use of composite materials in modern orthopaedic medicine and prosthetic devices: A review. Composites Sci. Technol. 2011, 71, 1791-1803.

47. Curran, S. A.; Ajayan, P. M.; Blau, W. J.; Carroll, D. L.; Coleman, J. N.; Dalton, A. B.; Davey, A. P.; Drury, A.; McCarthy, B.; Maier, S.; Strevens, A. A Composite from Poly(m-phenylenevinylene-co-2,5-dioctoxy-p-phenylenevinylene) and Carbon Nanotubes: A Novel Material for Molecular Optoelectronics. Adv Mater 1998, 10, 1091-1093.

48. Keshmiri, M.; Mohseni, M.; Troczynski, T. Development of novel TiO 2 sol–gel-derived composite and its photocatalytic activities for trichloroethylene oxidation. Applied Catalysis B: Environmental 2004, 53, 209-219.

49. Bascom, W. & Drzal, L. The Surface Properties of Carbon Fibre and their Adhesion to Organic Polymers. 1987.

50. Chua, P. S. Dynamic mechanical analysis studies of the interphase. Polymer Composites 1987, 8, 308-313.

51. Dry, C. M.; Sottos, N. R. Passive smart self-repair in polymer matrix composite materials. Smart Structures and Materials 1993: Smart Materials 1993.

52. White, S. R.; Sottos, N. R.; Geubelle, P. H.; Moore, J. S.; Kessler, M. R.; Sriram, S. R.; Brown, E. N.; Viswanathan, S. Autonomic healing of polymer composites. Nature 2001, 409, 794-797.

53. Wool, R. P. Self-healing materials: a review. Soft Matter 2008, 4, 400.

54. Chiari, G.; Giustetto, R.; Druzik, J.; Doehne, E.; Ricchiardi, G. Pre-columbian nanotechnology: reconciling the mysteries of the maya blue pigment. Applied Physics A 2008, 90, 3-7.

55. Schadler, L. S. Polymer-Based and Polymer-Filled Nanocomposites. Nanocomposite Science and Technology 2014, 77-153.

56. Novak, B. M. Hybrid Nanocomposite Materials - between inorganic glasses and organic polymers. Adv Mater 1993, 5, 422-433.

57. Edser, C. Auto applications drive commercialization of nanocomposites. Plastics, Additives and Compounding 2002, 4, 30-33.

58. Westbroek, P.; Marin, F. A marriage of bone and nacre. Nature 1998, 392, 861-862.

59. Heinemann, F. Bruchfläche eines Perlmuttstücks. https://commons.wikimedia.org/wiki/File:Bruchfl%C3%A4che_eines_Perlmuttst%C3%BCcks.JPG (accessed May 01, 2016).

60. Kebes Nacre microscopic structure. https://commons.wikimedia.org/wiki/File:Nacre_microscopic_structure.png.

61. Bakshi, S. R.; Lahiri, D.; Agarwal, A. Carbon nanotube reinforced metal matrix composites - a review. International Materials Reviews 2010, 55, 41-64.

62. Lalwani, G.; Henslee, A. M.; Farshid, B.; Lin, L.; Kasper, F. K.; Qin, Y.; Mikos, A. G.; Sitharaman, B. Two-Dimensional Nanostructure-Reinforced Biodegradable Polymeric Nanocomposites for Bone Tissue Engineering. Biomacromolecules 2013, 14, 900-909.

63. Morgan, A. B.; Wilkie, C. A., Eds.; In Flame Retardant Polymer Nanocomposites; John Wiley & Sons, Inc.: 2007; .

64. Singh, B. P.; Singh, D.; Mathur, R. B.; Dhami, T. L. Influence of Surface Modified MWCNTs on the Mechanical, Electrical and Thermal Properties of Polyimide Nanocomposites. Nanoscale Res Lett 2008, 3, 444-453.

65. Hussain, F. Review article: Polymer-matrix Nanocomposites, Processing, Manufacturing, and Application: An Overview. J. Composite Mater. 2006, 40, 1511-1575.

66. Alemán, J. V.; Chadwick, A. V.; He, J.; Hess, M.; Horie, K.; Jones, R. G.; Kratochvíl, P.; Meisel, I.; Mita, I.; Moad, G.; Penczek, S.; Stepto, R. F. T. Definitions of terms relating to the structure and processing of sols, gels,

networks, and inorganic-organic hybrid materials (IUPAC Recommendations 2007). Pure and Applied Chemistry 2007, 79, 1801-1829.

67. Sperling, L. H. Interpenetrating Polymer Networks: An Overview. In Interpenetrating Polymer Networks; Klempner, D., Sperling, L. H. and Utracki, L. A., Eds.; American Chemical Society: Washington, D.C., 1994; pp 3-38.

68. Roland, C. M. Interpenetrating Polymer Networks (IPN): Structure and Mechanical Behavior. Encyclopedia of Polymeric Nanomaterials 2013, 1-9.

69. Dragan, E. S. Design and applications of interpenetrating polymer network hydrogels. A review. Chem. Eng. J. 2014, 243, 572-590.

70. Peterson, A. M.; Kotthapalli, H.; Rahmathullah, M. A.; Palmese, G. R. Investigation of interpenetrating polymer networks for self-healing applications. Composites Sci. Technol. 2012, 72, 330-336.

71. Chen, C.; Xiong, C.; Yang, J.; Dong, L. Microstructure and properties of fluoroelastomer/butadiene-acrylonitrile rubber interpenetrating polymer networks. Journal of Wuhan University of Technology-Mater. Sci. Ed. 2008, 23, 50-53.

72. P., B.; H., S.; X., N.; Q., P. All-silicone prestrain-locked interpenetrating polymer network elastomers: free-standing silicone artificial muscles with improved performance and robustness. Smart Material Structures 2013, 22, 055022.

73. Hager, M. D.; Greil, P.; Leyens, C.; van, d. Z.; Schubert, U. S. Self-Healing Materials. Adv Mater 2010, 22, 5424-5430.

74. Wu, D. Y.; Meure, S.; Solomon, D. Self-healing polymeric materials: A review of recent developments. Progress in Polymer Science 2008, 33, 479-522.

75. Jud, K.; Kausch, H. H.; Williams, J. G. Fracture mechanics studies of crack healing and welding of polymers. J. Mater. Sci. 1981, 16, 204-210.

76. Guimard, N. K.; Oehlenschlaeger, K. K.; Zhou, J.; Hilf, S.; Schmidt, F. G.; Barner-Kowollik, C. Current Trends in the Field of Self-Healing Materials. Macromol.Chem.Phys. 2011, 213, 131-143.

77. Wool, R. P. A theory of crack healing in polymers. J. Appl. Phys. 1981, 52, 5953.

78. Silverstein, R. M.; Bassler, G. C.; Morrill, T. C. Spectrometric identification of organic compounds; John Wiley & Sons: Canada, 1991; .

79. Zhao, X. A theory for large deformation and damage of interpenetrating polymer networks. Journal of the Mechanics and Physics of Solids 2012, 60, 319-332.

Appendix A – NMR Spectroscopy Result of Functionalized Polyketones

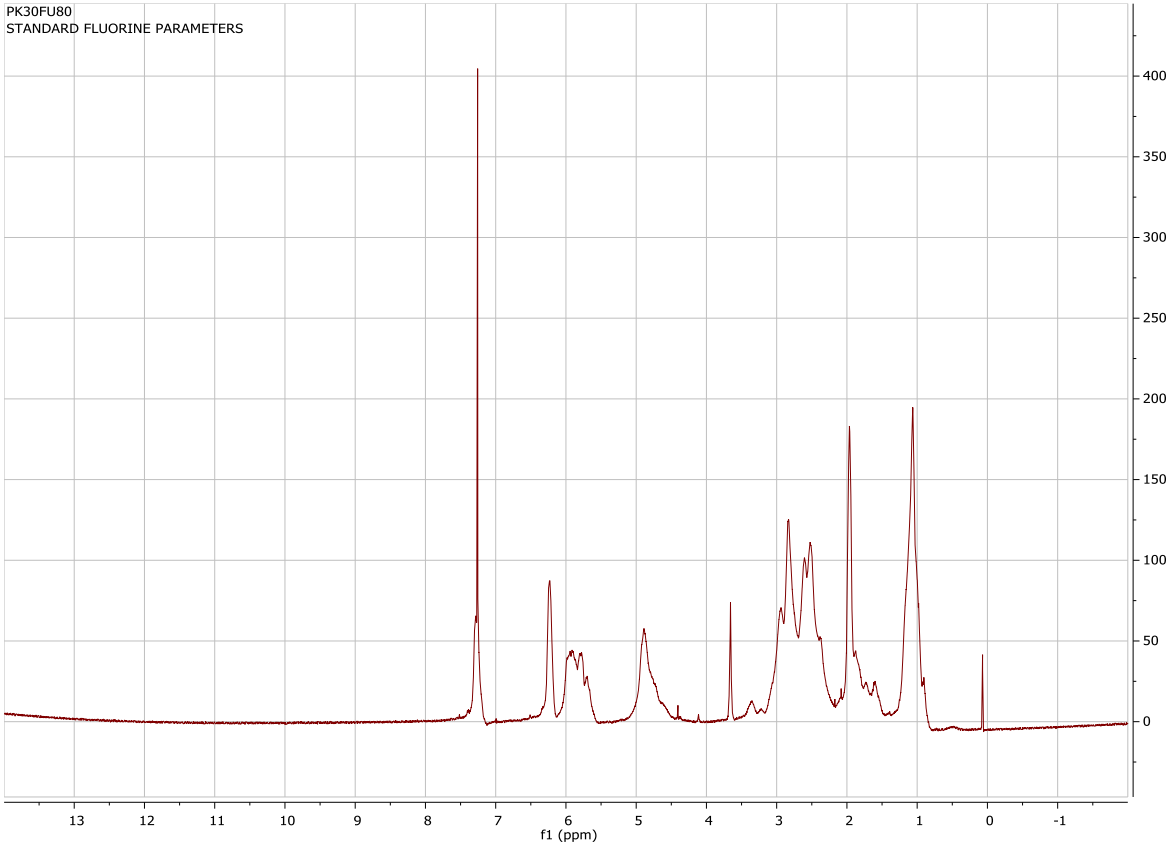

Figure 25. ^{1}H NMR Spectrogram of polyketone functionalized with furfurylamine at 80% conversion.

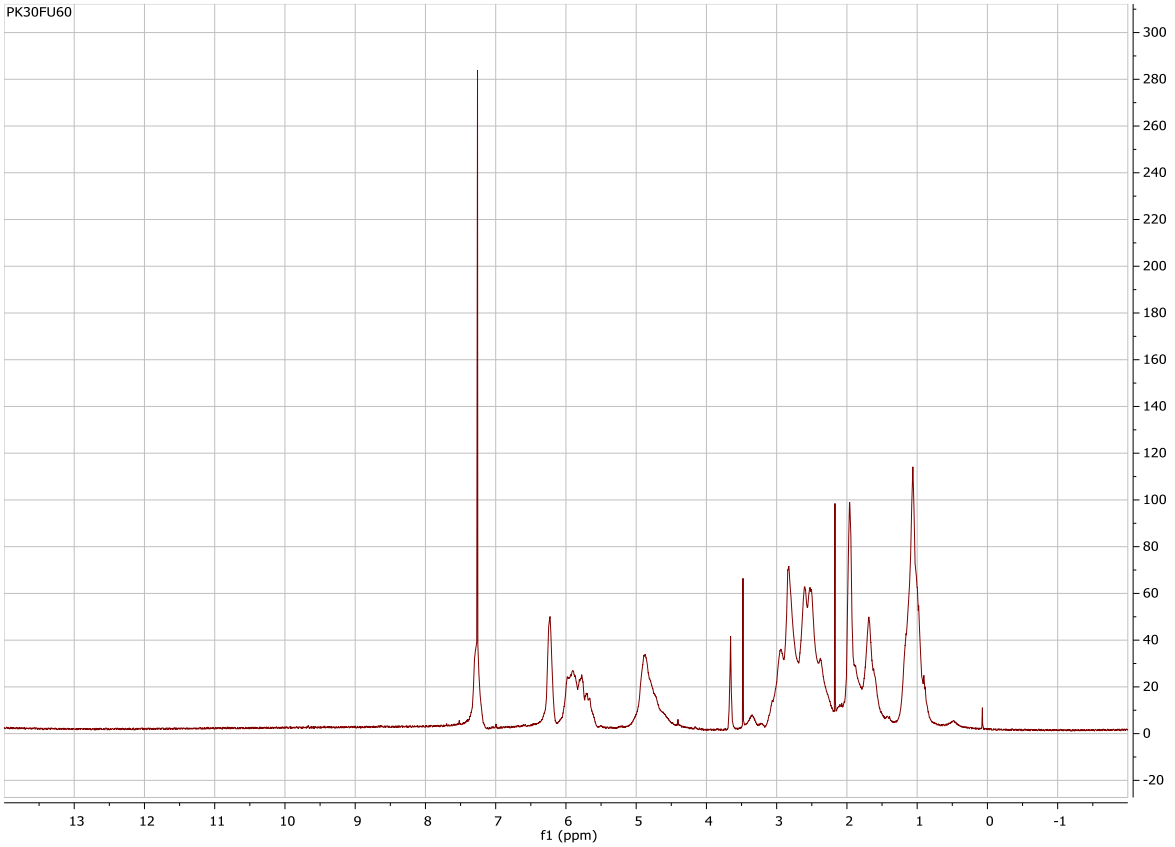

Figure 26. ^{1}H NMR Spectrogram of polyketone functionalized with furfurylamine at 60% conversion.

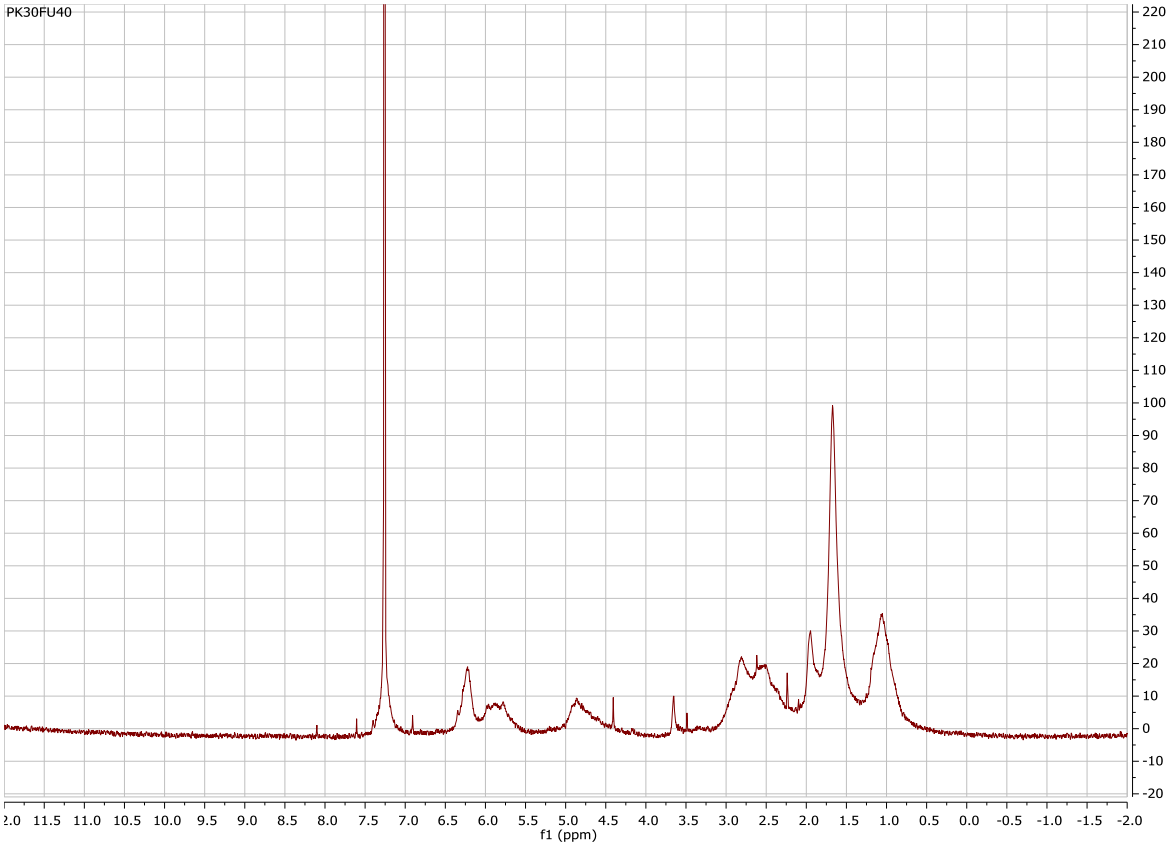

Figure 27. ^{1}H NMR Spectrogram of polyketone functionalized with furfurylamine at 40% conversion.

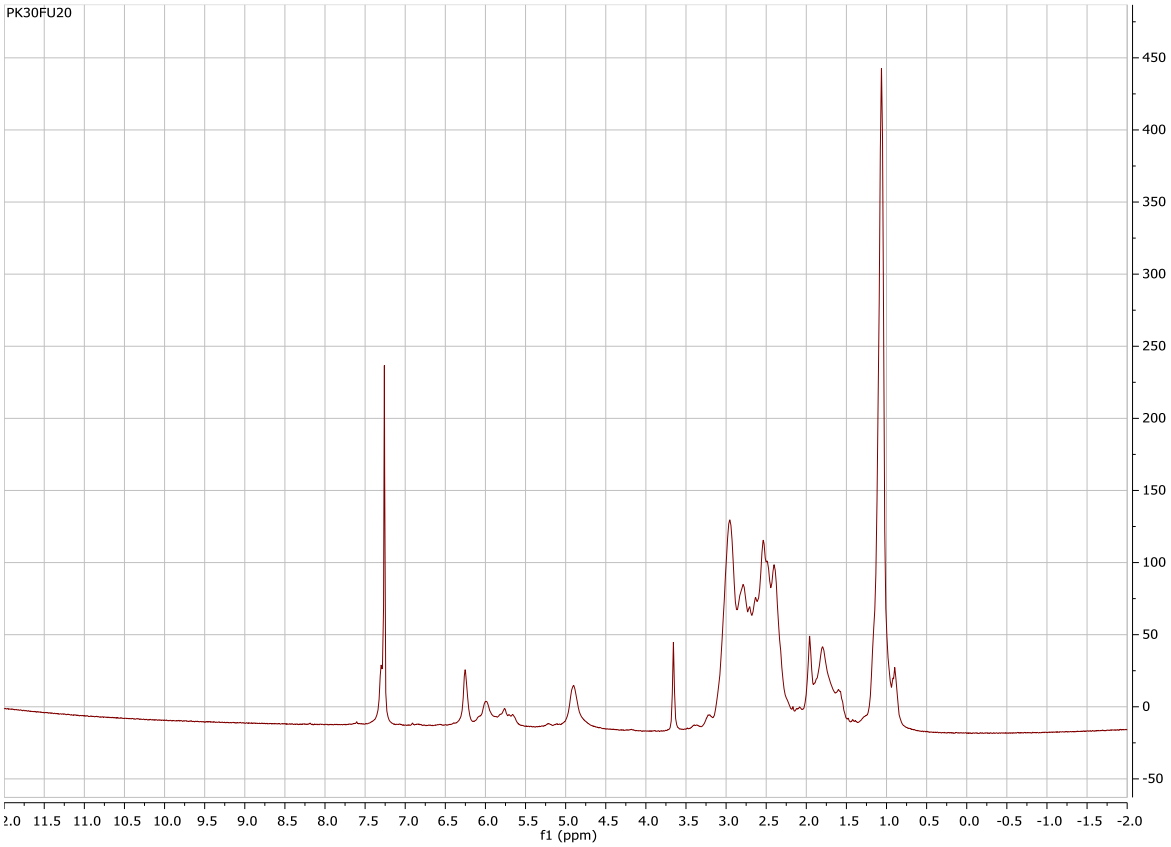

Figure 28. ^{1}H NMR Spectrogram of polyketone functionalized with furfurylamine at 20% conversion.

Appendix B – ATR-FTIR Spectra of Functionalized Polyketones

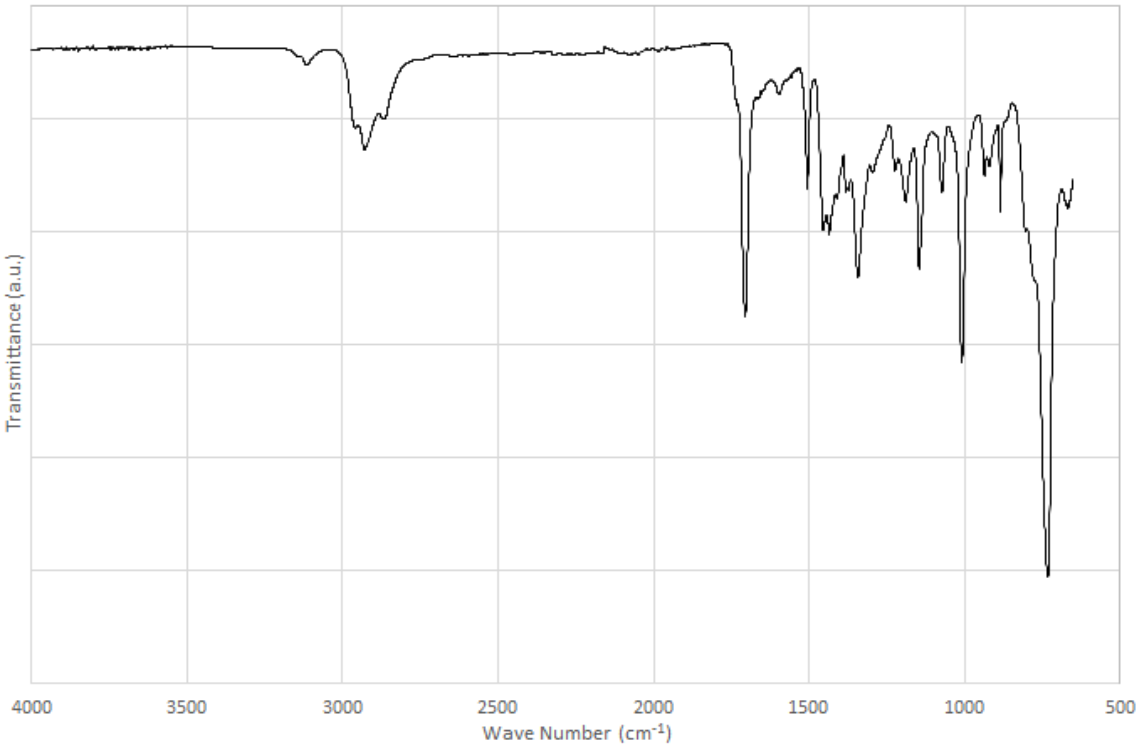

Figure 29. ATR-FTIR spectrogram of PK30FU80.

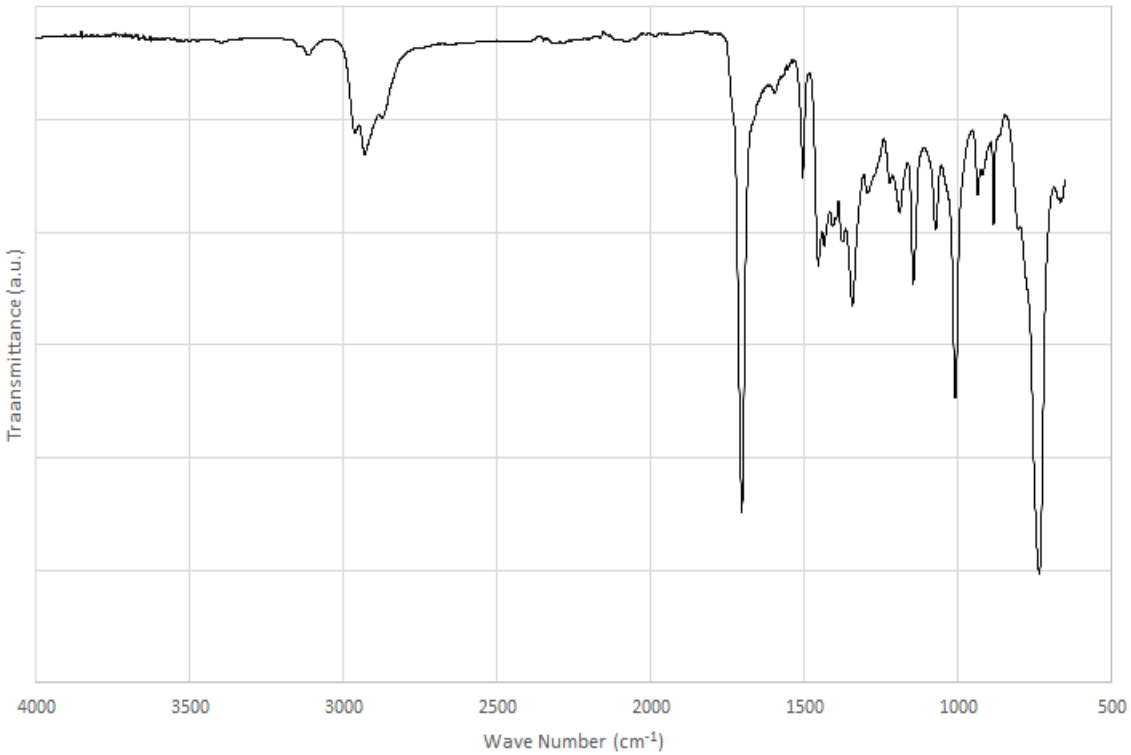

Figure 30. ATR-FTIR spectrogram of PK30FU60.

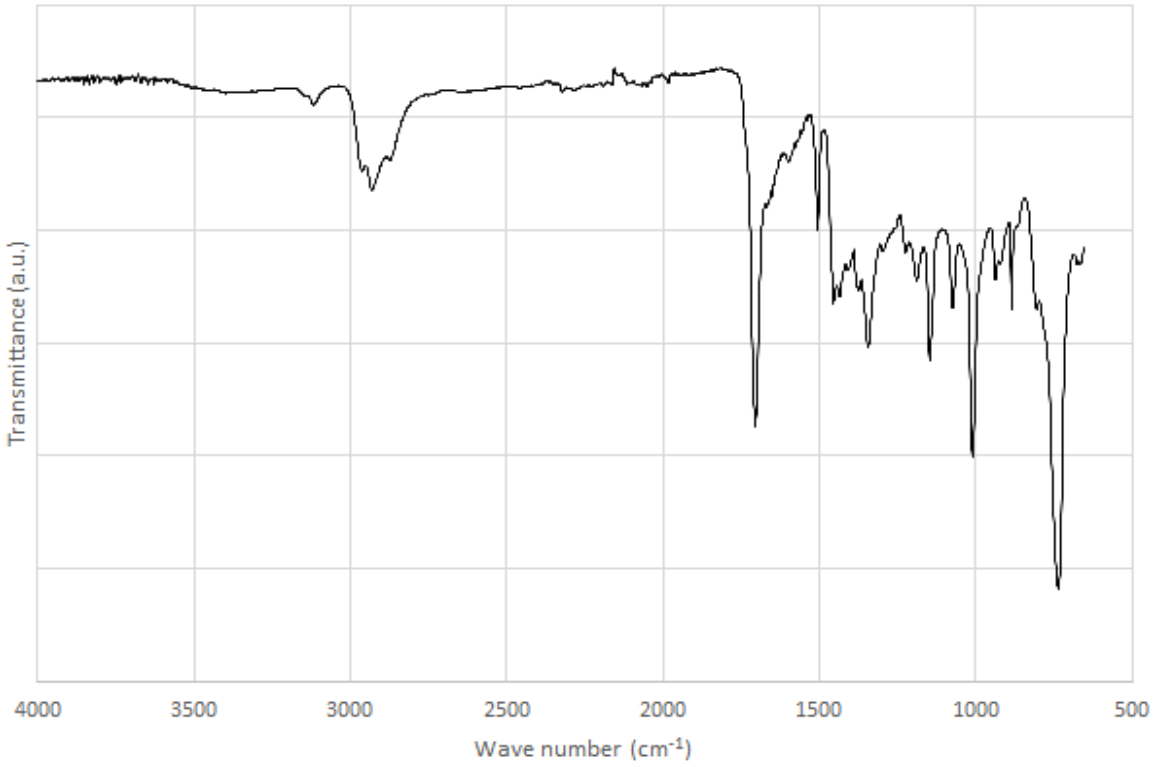

Figure 31. ATR-FTIR spectrogram of PK30FU40.

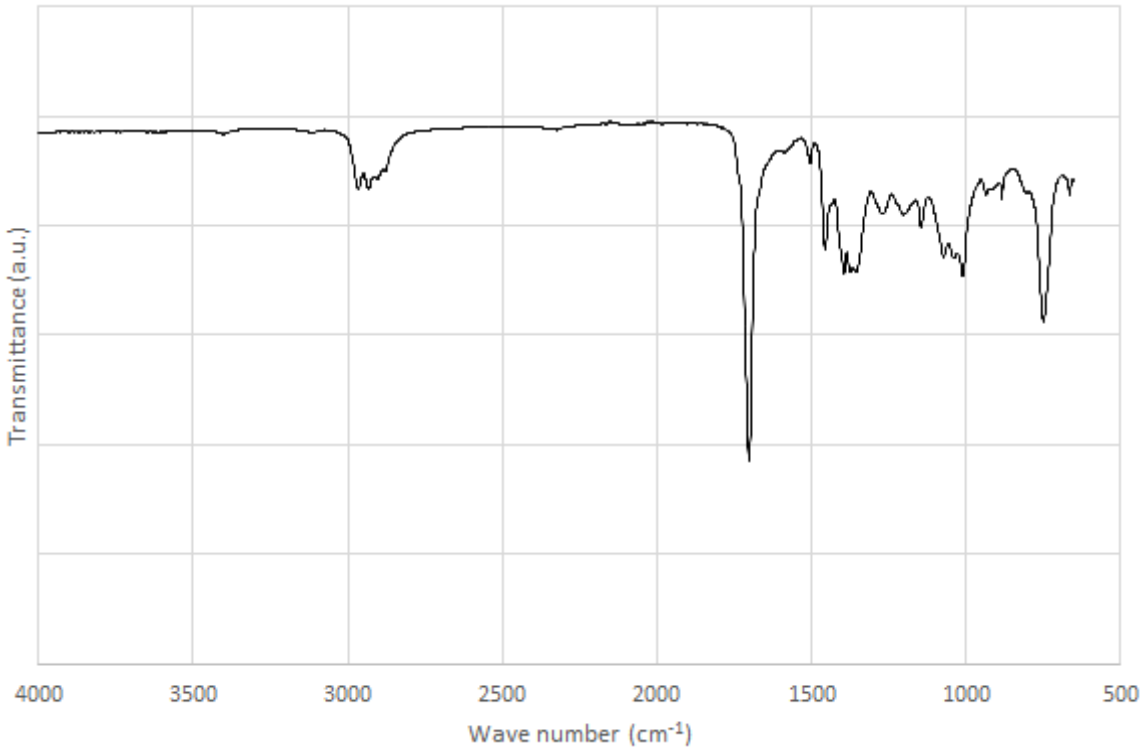

Figure 32. ATR-FTIR spectrogram of PK30FU20.